SEAWATER ALTERATION OF PILLOW LAVAS, BAY OF ISLANDS OPHIOLITE COMPLEX, WESTERN NEWFOUNDLAND.

SEAWATER ALTERATION OF PILLOW LAVAS, BAY OF ISLANDS OPHIOLITE COMPLEX, WESTERN NEWFOUNDLAND

by

MICHAEL T. FRANKLYN

A Thesis

Submitted to the Department of Geology

in Partial Fulfillment of the Requirements

for the Degree

Bachelor of Science

McMaster University

April, 1985

BACHELOR OF SCIENCE (1985)

(Geology)

McMaster University
Hamilton, Ontario

Title : Seawater alteration of pillow lavas, Bay of Islands ophiolite complex, western Newfoundland.

Author: Michael T. Franklyn

Supervisor: Dr. R.H. McNutt

Number of pages: ix , 86

ABSTRACT

The pillow lavas of the lower Crabb Creek area of the Bay of Islands Ophiolite complex exhibit geochemical and petrographic characteristics similar to metamorphosed mid-ocean ridge basalts. Depletions of Ca and Mg and the enrichment of K, P, Na, Si and H_2O are the result of hydrothermal alteration and the metasomatic influence seawater on fresh basalts.

All samples exhibit typical low grade, greenschist facies metamorphic mineral assemblages. 'Fresh', moderately altered and severely altered suites can be recognized by the degree of degradation of the phenocryst and matrix phases. Immobile trace elements show these metabasalts to originally be ocean-floor tholeiites.

ACKNOWLEDGEMENTS

For suggesting this topic and introducing me to the area, I would like to sincerely thank Mark Langdon.

I express my appreciation to Dr. R.H. McNutt for his guidance, constructive advice, good humour and patience.

Thanks go also to Mr. O. Mudroch for his assistance and advice concerning chemical analyses and Mr. J. Whorwood and Mr. T. Bryner for their assistance in the preparation of the photographs found herein. Ms. J. Carson was a great help with an often troublesome SEM. Mr. L. Zwicker expertly prepared the thin sections used in this study.

For their advice and suggestions I would like to thank Andy Fyon, Ann Wilson and Tracey Hurley. My thanks also to Steve Davies and Steve Bonnyman for their assistance in the computer work involved in this thesis.

A special thanks goes to Karen Leblanc for her patience during the deciphering of the original manuscript from which this thesis was typed.

Finally, I would like to say thanks to my friends and the class of 1985 for making this a truly memorable past four years.

TABLE OF CONTENTS

LIST OF FIGURES

LIST OF PLATES

LIST OF TABLES

Plate 1: A view of North Arm Mountain (looking NE), just east of Stowbridge Head. The contact between the Humber Bay Supergroup and the overlying allochthonous ultramafic basal unit of the ophiolite is highlighted by the lack of vegetation on the rust-coloured harzburgite. Vertical relief approximately 650 metres.

CHAPTER ONE

INTRODUCTION

1.1 Purpose of Study

Detailed and exhaustive studies of the dynamothermal aureole and ultramaphic unit of the Bay of Islands Ophiolite Complex have been published (Malpas 1979, Williams and Smyth 1973), however, the pillow lava unit of this complex has not received the same intensive investigation. The purpose of this study was to undertake a detailed petrographic and geochemical study of the pillow lava unit as exposed in the Crabb Creek valley with the following objectives in mind:

1. To identify the degree and type of alteration present.
2. To identify geochemical trends and relate them to alteration.
3. To identify the tectonic environment in which this volcanic unit was emplaced.

1.2 Location and Accessibility

The thesis area is located within the pillow lava unit of the Bay of Islands Ophiolite Complex in Western Newfoundland (figure 1). It is located at military grid reference point 158601 on map sheet 12G/8. Its meridian and parallel location is 49°17 'N and 58°10 'W. The area is 55 km NNW of Corner Brook and 70 km East of Deer Lake. Due to the remoteness and rugged terrain of the Lower Crabb Creek Valley, access is only possible by helicopter.

1.3 Sampling

The thesis area consists of a single flat-lying outcrop on the north side of Crabb Creek approximately 800 metres upstream (east) of the confluence of Crabb Creek and Steep Brook (plate 2, also see map in sleeve at back). The outcrop is approximately 55 metres long and consists of well defined pillow lavas (plate 3) and an interpillow flow (plate 4) of variable thickness (5 cm to 70 cm). Sharp contacts are evident between the flow and the surrounding pillow (plate 5).

Figure 1: Simp[lified geological map of the Bay of Islands ophiolite complex.
(after Williams and Malpas 1972)

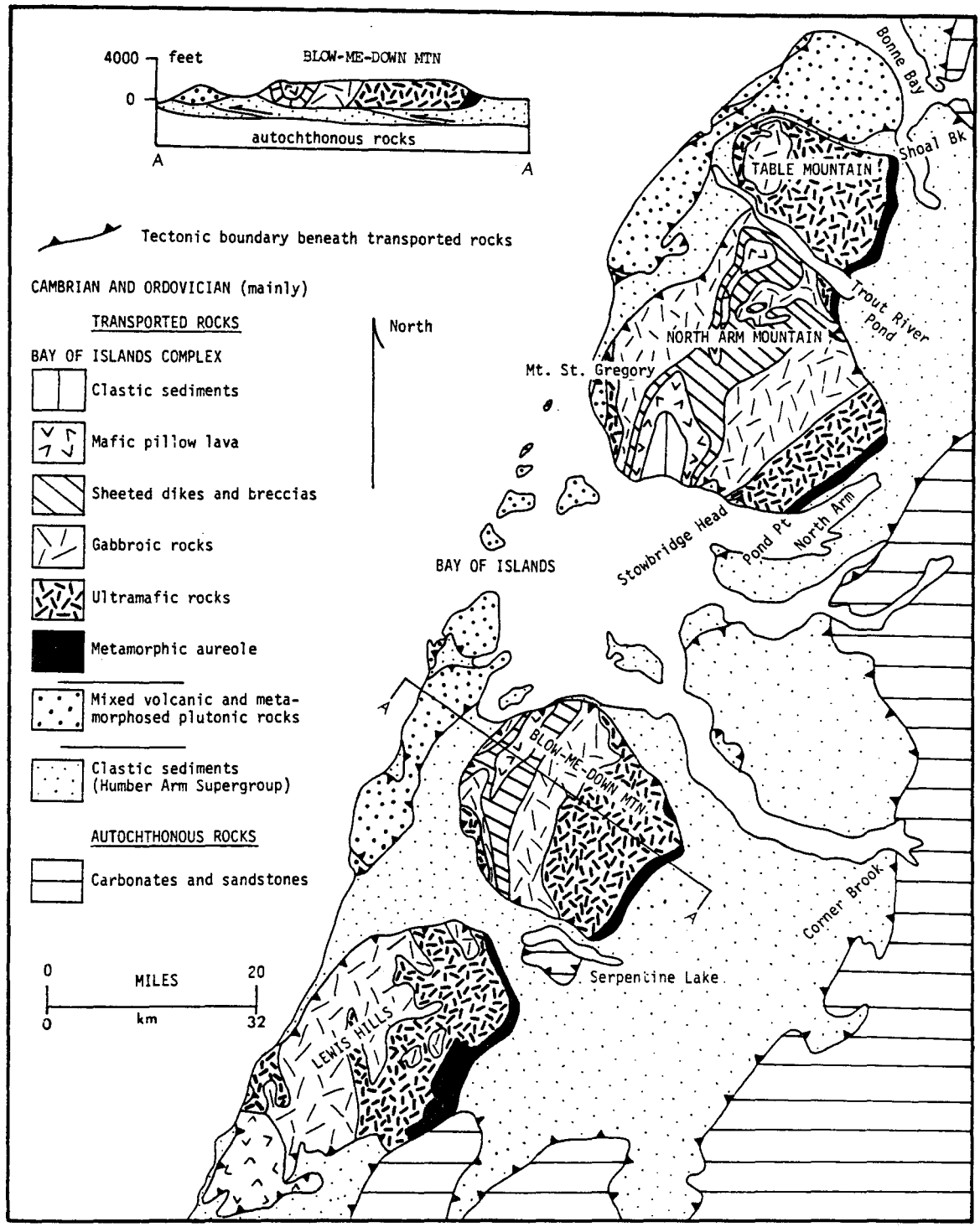

The geologic setting of the Bay of Islands Complex and the location and extent of its metamorphic aureole.

Plate 2: A photograph of the thesis outcrop, lower Crabb Creek. River is at very low stage but high water level is demarcated by base of trees behind outcrop. Outcrop is approximately 55 metres in length.

Plate 3: Well defined pillows in the thesis outcrop exhibiting radial and concentric fractures, probably due to cooling. Note Fe-stained oxidation rims. Approximate diameter of large pillow is 1 m.

Plate 4: A view of the gossaned inter-pillow flow. Note its variable thickness and sinuous nature.

Representative samples of both the 'flow' and the pillows were taken. The outcrop is submerged for several months each year and therefore extensive weathering is a problem (plate 6). Sampling was difficult due to the polished surfaces created by the river but, wherever possible, large samples were taken in an attempt to minimize the effects of this surface weathering. The weathered surfaces were later removed. Several samples however, when sectioned, were found to be unsuitable for further study due to their extensive weathering.

Due to time constraints, the author was unable to generate a map of the sampling area.

1.4 Previous Work

Prior to 1933 the mafic-ultramafic rocks of Western Newfoundland had been mapped on a reconnaissance basis only (Howley 1907). From 1933 to 1937 several workers outlined the general lithology and structure of the area. In 1958 Smith published the first detailed map of the area.

Plate 5: Very sharp contact between a green pillow (with hammer) and the inter-pillow flow which wraps around it. Note the abundance of fragments/ clasts in the flow.

Plate 6: Extensive surface weathering of a pillow. Weathering is enhanced by heavy fracturing in many pillows. Sample width is 30 cm.

Plate 7: Brecciation and shearing as seen in a hand sample of the inter-pillow flow. Sample width 30 cm.

Plate 8: Effects of hydrothermal alteration seen in hand sample. Silicification concentrated along veins with accompanying wallrock alteration. Sample width 15 cm.

Most early workers interpreted the Bay of Islands Complex as a layered autochthonous pluton and as such it was referred to in the literature as the Bay of Islands Igneous Complex until 1963. The work prior to this tended to concentrate primarily on the petrology, age and form of the plutons and their relationship with the surrounding rocks.

Johnston (1941) and Kay (1945) were the first to suggest that the clastic sedimentary rocks underlying the Bay of Islands Complex could represent a transported succession, equivalent in age to the underlying Cambrian-Ordoviocian carbonate sequence. Rodgers and Neale (1963) interpreted the mafic-ultramafic complex as well as the underlying clastics as part of a transported terrane. Stevens (1970), based upon field relationships and the presence of chromite grains and pyroxene crystals in the clastic sequence, suggested that the clastic sediments and the mafic-ultramafic complex represented separate thrust sheets and that in fact, the mafic-ultramafic complex was a possible source terrain for the easterly derived sedimentary debris. Stevens (1970) was the first to suggest that perhaps this transported sequence could represent ocean crust, and might possibly be related to the opening and closing of the proto-Atlantic (Wilson,1966).

Based upon the recognition of extensive sheeted dikes bounded by gabbroic rocks below and pillow lavas above at Blow-Me-Down Mountain, Williams and Malpas (1972) interpreted the Bay of Islands Complex as representing a a typical ophiolite suite. Subsequent work on the Bay of Islands ophiolite complex, primarily by J. Malpas and H. Williams (Malpas 1977, 1978, Malpas and Talkington 1979, Williams 1971, 1972, 1973, 1978), has centred upon the emplacement tectonics, structural succession and the nature of the dynamothermal aureole that is found at the base of the ophiolite thrust sheet.

Casey and Kidd (1981) published a comprehensive study of the parallochthonous sediments that unconformably overlie the ophiolite complex.

The thesis area , just east (upstream) of the confluence of Steep Brook and Crabb Creek is not shown as a sample location and is not mentioned in any of the literature covered by this author. The pillow lava unit, within which the thesis area is located, is described only for exposures on Blow-Me-Down and North Arm Mountains (Malpas and Stevens 1977). Due to the inaccessibility of the Lower Crabb Creek Valley, the area between Mt. St. Gregory to the north and North Arm

Mountain to the south has been mapped mostly on the basis of air photo interpretation. Unpublished maps by Duval Intl. Corp., based upon three field seasons in the Lower Crabb Creek area, provide the most detail lithological information on the area (see map inside back cover).

1.5 Background

Ophiolites

Steinmann (1905), Benson (1926) and other early workers interpreted ophiolites as the intrusive and volcanic products of eugeosynclinal environments that were later involved and incorporated during a period of orogenesis. This interpretation was based upon their work in the Alps. However, with the introduction of the theory of plate tectonics, ophiolites were re-examined from a new perspective. Interpreted as segments of oceanic lithosphere by several workers (Dietz 1963, Hess 1964, Dewey and Bird 1971) the investigation of ophiolites took on a new importance.

The term 'ophiolite' is frequently misused. From the 1972 Penrose Conference on ophiolites came the definition of an ophiolite as a distinctive assemblage of mafic to ultramafic rocks. The word 'ophiolite' should not be used as a rock name or as a lithologic unit in mapping. A completely developed ophiolite consists of the following rock types occurring in the order (from bottom to top); ultramafic complex, gabbroic complex, mafic sheeted dike complex, mafic volcanic complex (Coleman 1977).

1.5.1 Ocean Crust

Based upon data from siesmic refraction measurements and sampling (dredge hauls) of the ocean floor and especially ridge-crests, Cann (1970) constructed a model of the structure of the oceanic crust and the way in which it formed at mid-ocean ridges. In this model Cann (1970) envisaged a zone or layer of unmetamorphosed pillow lavas that can be divided into two distinct metamorphic zones. The lower unit has undergone greenschist metamorphism while the upper lava unit has undergone only zeolite facies metamorphism with the accompanying development of clay minerals from ferromagnesium minerals.

The pillow lavas are in turn intruded from below by feeder dikes which supply the extrusive flows. The diabase dike swarms grade downwards into a massive, layered, coarse-grained gabbroic unit which forms the base of the crust.

In his model, Cann (1970) did not compare this 'deduced' ocean crust structure to any on-land ophiolites. However, several ophiolite suites, including the Bay of Islands complex, show exactly this sequence of rock types.

1.5.2 Upper Mantle

Based upon inclusions in basalts from oceanic islands, geographical evidence and ophiolite analog studies, the mantle underlying the oceanic crust can be divided into three components (Coleman 1977):

i) Primitive mantle - a lherzolite or garnet peridotite thought to represent primitive, undepleted mantle material.

ii) Depleted mantle - typically a tectonized harzburgite, the residua of the partial melting (up to 30%) of primitive mantle material from which the tholeiitic basalts are thought to be generated.

iii) Cumulate ultramafics - dunites and pyroxenites thought to be formed by the fractionation of the magma produced by partial melting.

Malpas (1977) recognized the genetic distinction between rocks formed in the mantle and those formed in the crust. Based upon differences in textures,

mineralogy and chemistry between the mafic volcanics and the underlying ultramafics, Malpas renamed this transitional 'Critical Zone' of Smyth (1958), the 'petrological Moho' to distinguish it from the 'seismic Moho' which occurs above it.

CHAPTER TWO

GENERAL GEOLOGY

2.1 The Bay of Islands Ophiolite Complex

2.1.1 Regional Geology

Four main groups of rocks can be recognized in Western Newfoundland; a Precambrian crystalline basement, an autochthonous sedimentary sequence, an easterly transported allochthonous sequence of sediments and a series of Cambrian-Ordovician autochthonous ophiolites (Bay of Islands and Hare Bay) and their associated sediments (Williams 1978).

The Bay of Islands ophiolite complex represents the major ophiolite slice of the Humber Bay Allochthon. The complex forms a northwest-trending zone, 96 km x 24 km, and consists of four separate massifs which from north to south are, Table Mountain, North Arm Mountain, Blow-Me-Down Mountain and the Lewis Hills. Whether these massifs represent separate transported bodies or are the erosional remnants of a once continuous slice is unknown, but all occupy the same structural position within the allochthon (Williams 1975).

A completely developed ophiolite suite is displayed at Blow-Me-Down and North Arm Mountains. This consists of a basal ultramafic unit (lherzolite + harzburgite + cumulus dunite) with an attached dynamothermal amphibolitic aureole, overlain by gabbros, a sheeted dike complex, mafic pillow lavas and overlying clastic sedimentary rocks (Church 1972).

The rock units of the ophiolite sequence are disposed in synclines with northeast-trending subhorizontal axes and moderately to steeply dipping limbs, in the three northern massifs. The tectonic base of each massif is truncated by subhorizontal thrust faults (Williams and Smith 1973).

The thesis area is located within the pillow lava sequence, northwest of North Arm Mountain. The pillows in this area are sulfide bearing and lack siltstone interbeds. Therefore, based upon a direct comparison with the pillowed volcanics of Troodos as described by Malpas and Stevens (1977) it is postulated by this author that these pillowed basalts are near the bottom of the volcanic pile (lower pillow lava unit).

CHAPTER THREE

PETROGRAPHY

Basalts are extrusive igneous rocks composed of approximately equal amounts of plagioclase and clinopyroxene, often augite. Other minerals of importance include olivine and orthpyroxene with accessory magenetite, hematite, illmenite, apatite, quartz and glass.

3.1.1 Ocean Floor Basalts

Ocean floor basalts, are distinctive in both their morphology and petrography from subaerially extruded basalts. Massive flows, pillow lavas, pillow breccias and stratified hyalotuffs can occur in sequence or alone depending upon viscosity and lava supply (Bryan 1972).

Massive flows and pillow lavas show many of the same petrographic features. Both show distinct textural zonation from a coarse-grained centre or core outwards to a quenched glassy rim or margin. Submarine pillow lavas tend to have an outer glassy rim (selvedge) which grades inwards to a spherulitic zone, a flow-aligned plagioclase zone and an inner pillow core (Bryan 1972). The full development of this sequence will depend upon the size and cooling history of the individual pillow.

The degree of metamorphism of ocean floor basalts at the surface appears to be minimal. However, sub-seafloor basalt-seawater interaction and the resultant chemical and mineralogical changes that occur are well documented (Spooner and Fyfe 1973, Hart et al 1974, Bischoff and Dickson 1975). Sub-seafloor metamorphism and mass transfer are an integral part of the sea-floor spreading and ocean-ridge geothermal processes (Rona 1984, Spooner and Fyfe 1973).

Spilites are submarine metabasalts composed predominantly of albite and augite as well as a number of secondary metamorphic minerals such as chlorite, actinolite, epidote, prenhite and pumpellyite. This low grade, greenschist facies metamorphic assemblage is now accepted almost universally as the result of metasomatic alteration and hydrothermal metamorphism of ocean floor basalts (Hughes 1973).

Spilitization does not occur at the surface of the seafloor. Based upon experimental investigation, Bischoff and Dickson (1975) have postulated that effective spilitization can occur only when large volumes of seawater are reacted with fresh basalts at conditions of 200^{o} C and 500 bars pressure.

Although the primary mineralogy is often drastically altered, many primary textures are preserved during spilitization. Spilitic albite is the result of post magmatic replacement of labradorite (Coombs 1974). The ophitic and intersertal textures of the parent igneous rocks are often well preserved. Augite is the only ferromagnesium mineral which may survive spilitiztion.

3.2 Petrography of Thesis Area Samples

Mineralogy, textural preservation and degradation of the phenocryst/groundmass phases were investigated as possible criteria with which to determine the relative degree of alteration in the fifteen thin sections examined. The mineralogy of all samples reflects very low to low grade metamorphism.

Based upon petrographic examination, the samples were subdivided into 'fresh', moderately altered and severely altered suites.

3.2.1 'Fresh' Basalts

These rocks, although not pristine tholeiites, have

Plate 9: Subophitic and intersertal texture as seen in the 'fresh' basalts. PPL. Field of view 3.5 mm.

retained the majority of their original igneous textures and mineralogy. They are feldspar-augite phyric tholeiites and show classic examples of the subophitic enclosure (plate10) of turbid, skeletal to tabular plagioclase microphenocrysts (.2 to 1 mm in length). The plagioclase has undergone slight sericitization and exhibits 'swallow-tail' and 'belt-buckle' quench morphologies.

Augite is the predominant ferromagnesium mineral present. The fractured, subhedral, equant to tabular phenocrysts range in size from 0.1 to 2 mm and are relatively fresh and free of inclusions. Olivine is a minor phase (<2%) but the presence of this mineral is an indication of the 'freshness' of this rock.

A fine grained chlorite-rich matrix comprises a substantial portion of these thin sections. This chlorite is interpreted as the result of devitrification and recrystallization of original basaltic glass. Occupying the interstitices between plagioclase laths, the chlorite exhibits 'classic' intersertal texture (plate 11).

Circular, chlorite and carbonate filled amygdules,

Plate 10: Subophitic enclosure of plagioclase (p) laths in augite (a) grain. Note the chlorite (c) filled amygdule at left. XPL. Field of view 1.4 mm.

Plate 11: Intersertal texture in 'fresh' suite. Chlorite (c) light green with brown Fe-rich margin occupying interstitial spaces between plagioclase laths (p). Opaques are pyrite and leucoxene. PPL Field of view 1.4 mm.


p
a
C

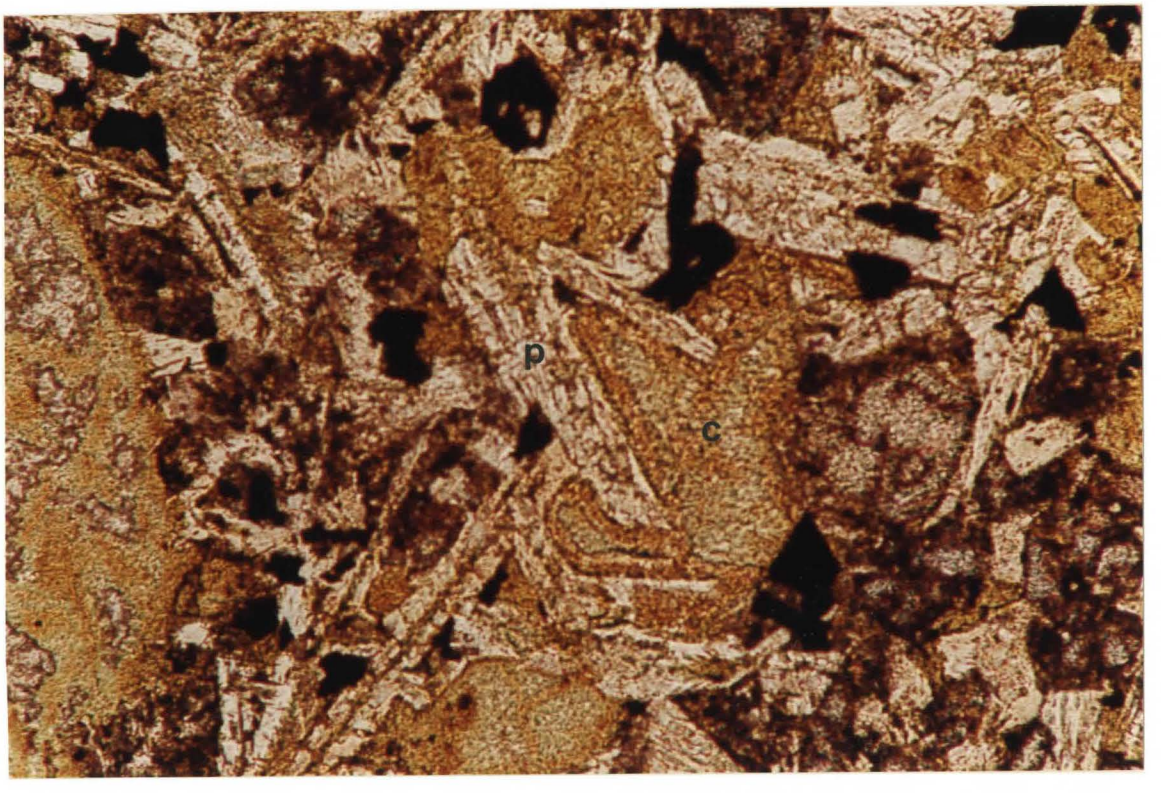
p
c

.2 to 1.8 mm in diameter, are often rimmed by opaques (plate12). Several of the amygdules contain 'wormy' intergrowths of penninite showing anomolous Berlin-blue interference colours (plate 13).

Leucoxene and granular sphene, common alteration products of Fe-Ti oxides, are ubiquitous in the groundmass, along with minor pyrite.

3.2.2 Moderately Altered Suite

The plagioclase phenocrysts of this suite have undergone considerable sericitization and saussuritization. The cloudy plagioclase laths have serrate, irregular outlines (plate14). Abundant sericite, zoisite and calcite inclusions are the products of saussuritization (hydrothermal alteration) of a more calcic plagioclase. Relic Carlsbad and albite twins, as well as minor sector zoning is apparent. Quench textures are not as abundant as in the previous suite. Intersertal texture is exhibited by the the chlorite (devitrified glass) and plagioclase.

The ferromagnesium minerals (cpx + olivine) have

Plate 12: Two circular amygdules infilled with chlorite (c) and calcite (cc). Note opaques (o) rimming both amygdules. Note also preservation of highly birefringent augite. Diameter of large amygdule 1.4 mm. XPL

Plate 13: Chlorite (c) filled amygdule (.7 mm in diameter) with Berlin-blue penninite (p) intergrowths. Dark brown semi-opaque grains are leucoxene (l). XPL

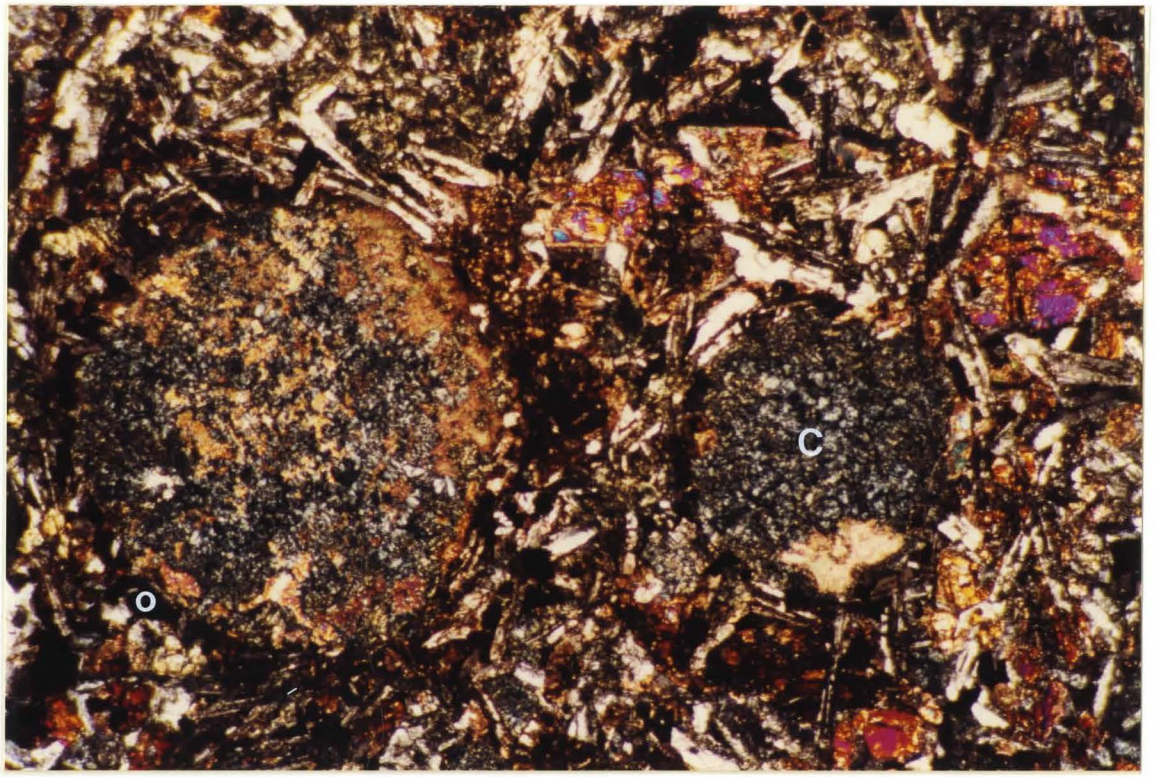
C
o

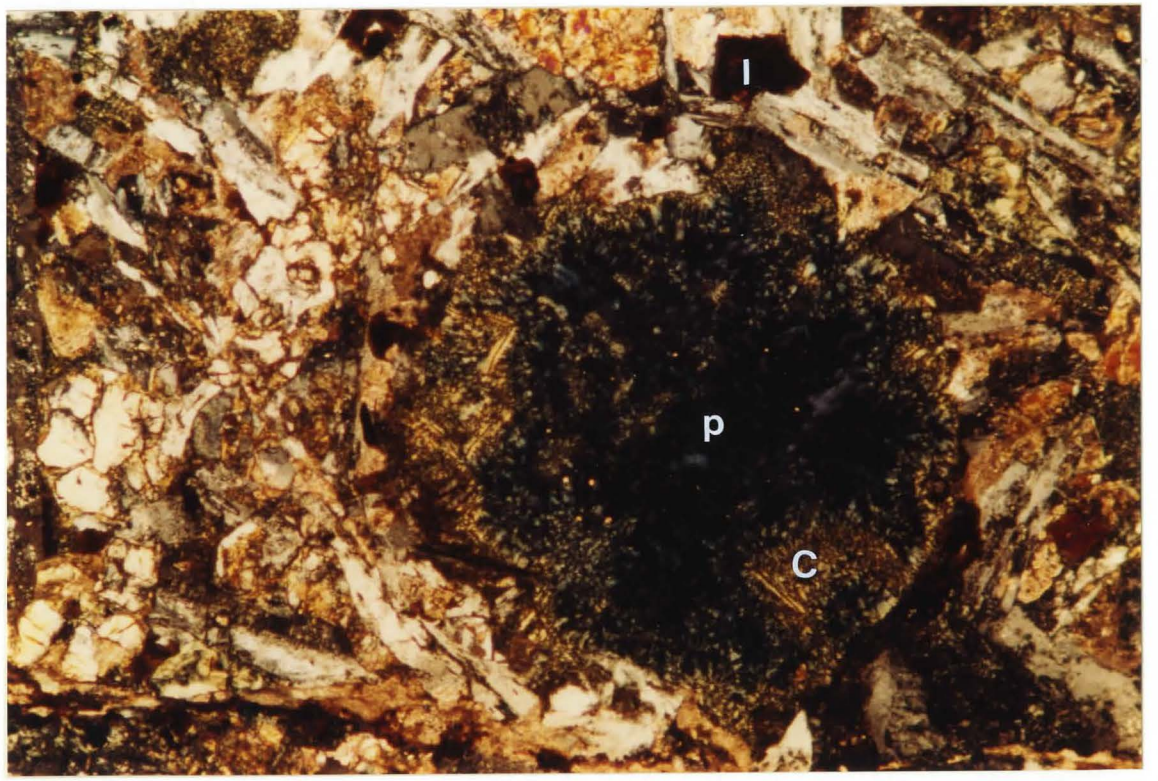
I
p
C

Plate 14: Photomicrograph of a typical example of the moderately altered suite showing irregular outline of plagioclase laths. Note the absence of augite in this slide and relative abundance of opaques. XPL. Field of view 1.4 mm.

Plate 15: Quartz-pyrite vein in moderately altered suite. Note the quartz overgrowths on euhedral pyrite. Fe-oxides line the vein and chlorite (c) has replaced basaltic glass (?). Evidence of saussauritization is seen in plagioclase above the vein with calcite and clinozoisite (z) inclusions. However, alteration of immediate wall rock is minimal. Vein width .3 mm. XPL


Z
C

been completely altered to a very fine-grained mixture of epidote, calcite, quartz, chlorite and abundant sphene.

Pyrite with quartz overgrowths and Fe-oxide alteration rims is concentrated within shear zones and veinlets (plate 15).

These samples are non-vesicular and many appear in outcrop to be pillow or flow breccias. Angular to sub-rounded, fine to medium-grained 'fragments' of basaltic composition are set in a very fine-grained, quartz and pyrite rich matrix (plate 16,17).

3.2.3 Severly Altered Suite

A bimodal size distribution of plagioclase and the complete alteration of the ferromagnesium minerals characterizes the severly altered suite.

Glomeroporphyritic texture is represented by clusters of large tabular plagioclase phenocrysts (glomerocryst diameters are .6 to 4.0 mm) (plate 19). Plagioclase is also present as very delicate, skeletal microlites (plate 20). Whispy, 'swallow tails',

Plate 16: Rounded basaltic fragments separated by quartz and pyrite rich matrix. XPL. Field of view 1.4 mm.

Plate 17: Photomicrograph showing rounded, fine-grained basaltic fragments found in the flow. Note the variation in fragment size. XPL Field of view 1.4 mm.

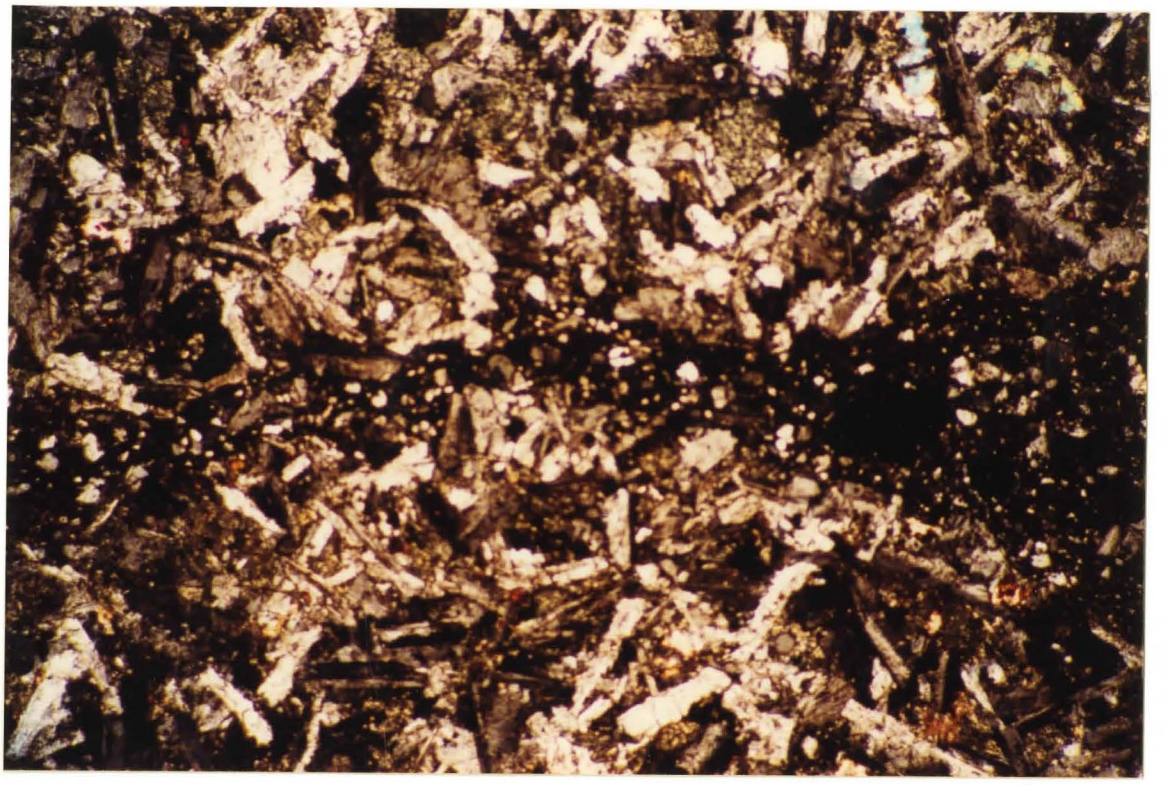

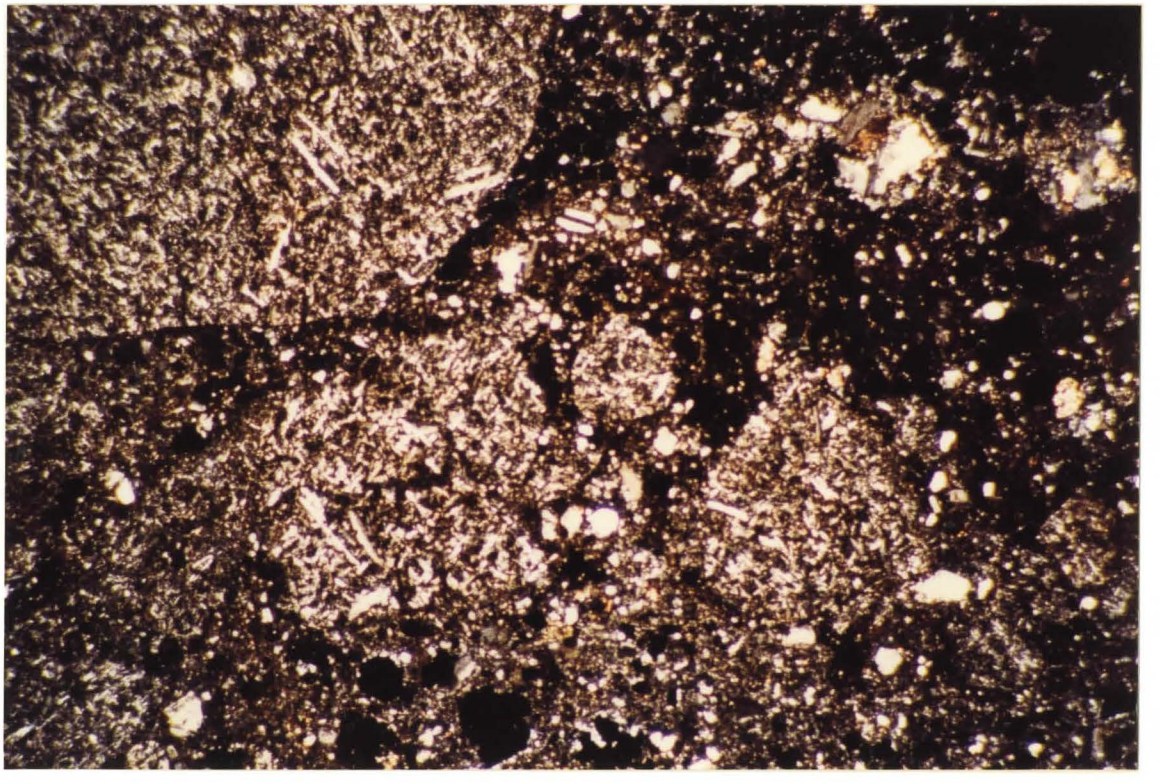

Plate 18: Flow aligned plagioclase microlites. XPL. Field of view 1.4 mm.

Plate 19: Glomeroporphyritic texture in severely altered suite. Cluster of large tabular plagioclase laths set in a matrix of very fine plagioclase microlites. Note the abundance of inclusions in the glomerocrysts and the very fine grained groundmass. XPL. Field of view 3.5 mm.

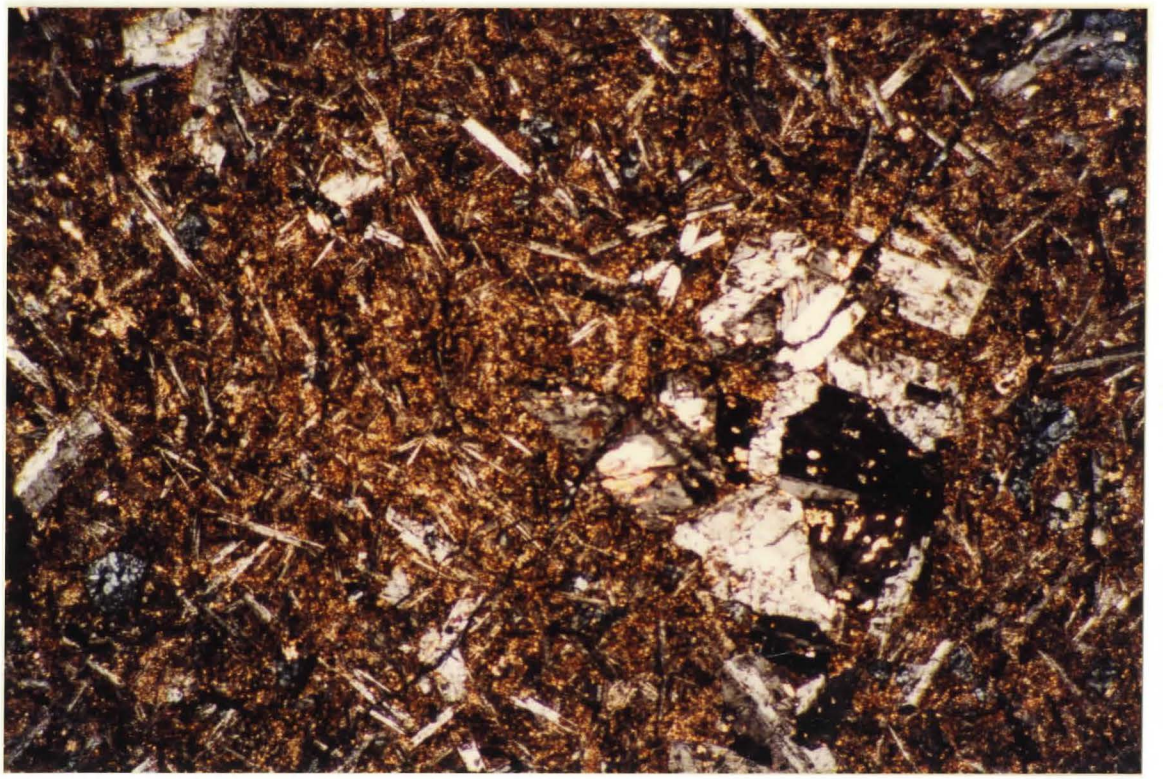

'belt-buckle', and spherulitic microlites are all quench crystal morphologies indicative of supercooling (plate 21). The bimodal size distribution of plagioclase, commonly seen in oceanic basalts, is produced by a sudden drop in temperature which induces supercooling. The result is a mixture of earlier formed tabular laths and quenched, skeletal microlites (Lofgren 1977).

Although textural preservation is excellent, all plagioclase has undergone extensive alteration. The cores of quenched microlites are invariably filled with cryptocrystalline groundmass material, calcite and chlorite. The large, tabular plagioclase phenocrysts areriddled with epidote, zoisite, chlorite and carbonate inclusions.

The groundmass is a very fine-grained mixture of the ferromagnesium alteration products; epidote, calcite, chlorite, sphene plus leucoxene and illmenite.

Several distinctly euhedral psuedomorphs of serpentine after olivine are present in these slides (plate 22). Central glass inclusions, now devitrified, contain epidote and opaques.

Circular amygdules (.2 to .5 mm in diameter) are filled with chlorite, calcite and opaques (plate23).

Plate 20: Delicate skeletal, swallow tail plagioclase microlites riddled with inclusions. PPL. Field of view 1.4 mm.

Plate 21: Belt buckle (b), spherulitic (s) and swallow tail (t) quench morphologies exhibited by skeletal plagioclase in severely altered suite. This plate exemplifies the preservation of delicate primary textures in a completely recrystallized matrix. XPL. Field of view 1.4 mm.


t
s
b

Plate 22: Serpentine (s) psuedomorphs after olivine. Distinct hexagonal cross-section of olivine is apparent. Oval inclusion (originally glass ?) now contains epidote, sphene and opaques. Possible iddingsite (?) as alteration product of Fe-oxides along fractures. Note abundance of inclusions in plagioclase glomerocryst to the left and tangentially oriented swallow tail microlites. XPL. Field of view 1.4 mm.

Plate 23: Circular amydule containing highly birefringent prenhite (p)?, chlorite (c) and opaques (o). XPL. Vesicle diameter 250 microns.


S


C
p
o
o

The abundance of opaques, especially pyrite, is considerably lower than in the previous two suites.

3.3 Ore Petrography

Pyrite is the primary ore mineral in polished sections. Minor amounts of sphalerite, chalcopyrite, magnetite, hematite and arsenopyrite are also seen.

Pyrite is concentrated along with quartz in veinlets that show no wall rock alteration. Individual veinlets show zoning with crustification banding in which the sulfides occur at the centre and the quartz and chlorite along the vein walls (plate 15). Desseminated pyrite is often abundant in the adjacent host rock. Vein pyrite is often euhedral. Small lenses of sulfides (plate 24) and pyrite stringers (plate 25) are seen in outcrop.

The most distinctive feature of the pyrite is its strong anisotropism. The anisotropism and twinning in pyrite are likely the result of stress induced

Plate 24: Small isolated lens of friable sulphides within the inter-pillow flow.

Plate 25: Hand sample showing the extent of fracturing and development of quartz-sulphide veins in the severely altered suite. Sample diameter 20 cm.

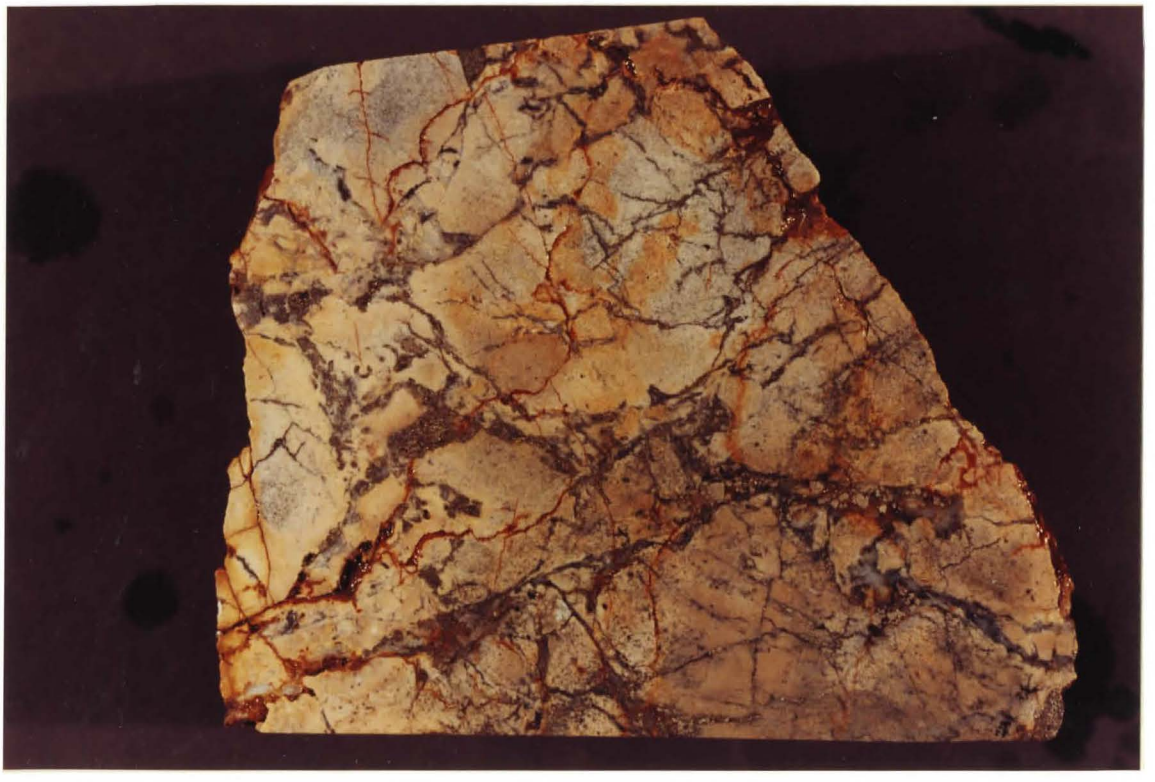

Plate 26: Brittle deformation and cataclastic texture in pyrite. All ore in field of view is pyrite, colours are not accurate. PPL. Field of view 1.5 mm.

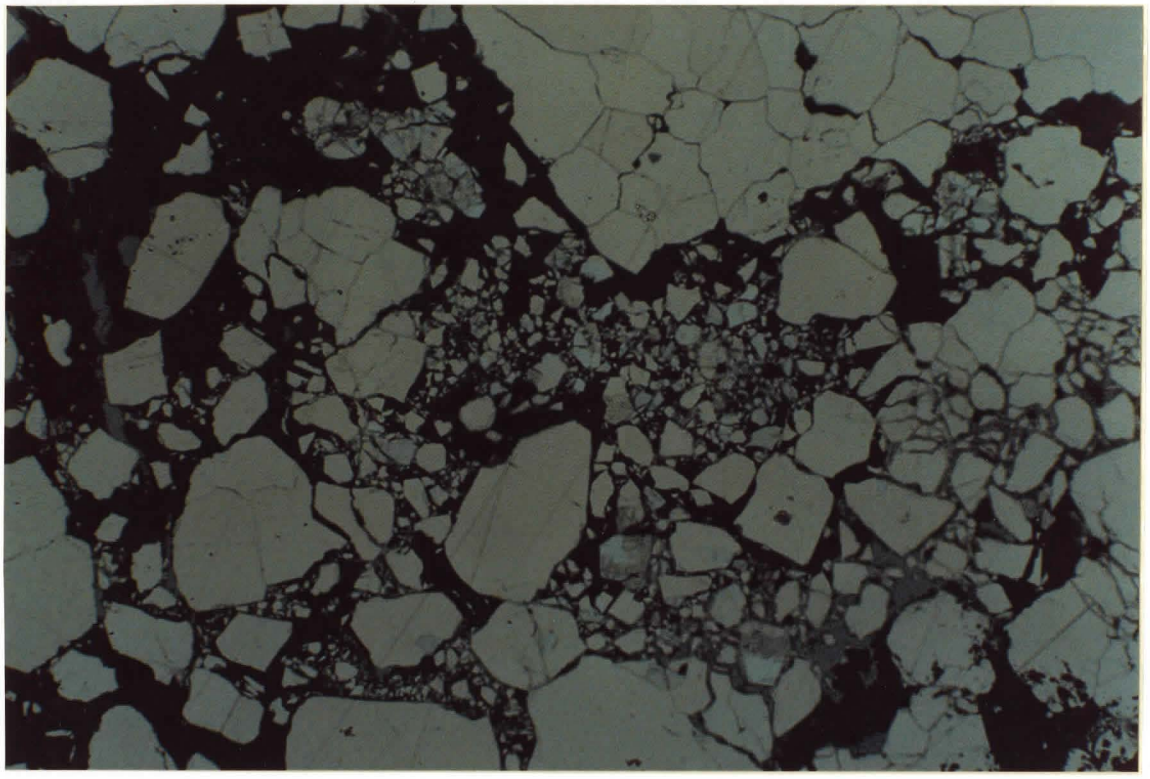

Plate 27: Large idioblastic pyrite crystal (top) in contact with recrystallizing (?) mass of tabular pyrite. PPL. Field of view 1 mm.

Plate 28: Same picture as above under crossed nicols. Strong anisotropism and twinning seen in pyrite. XPL. Field of view 1 mm.

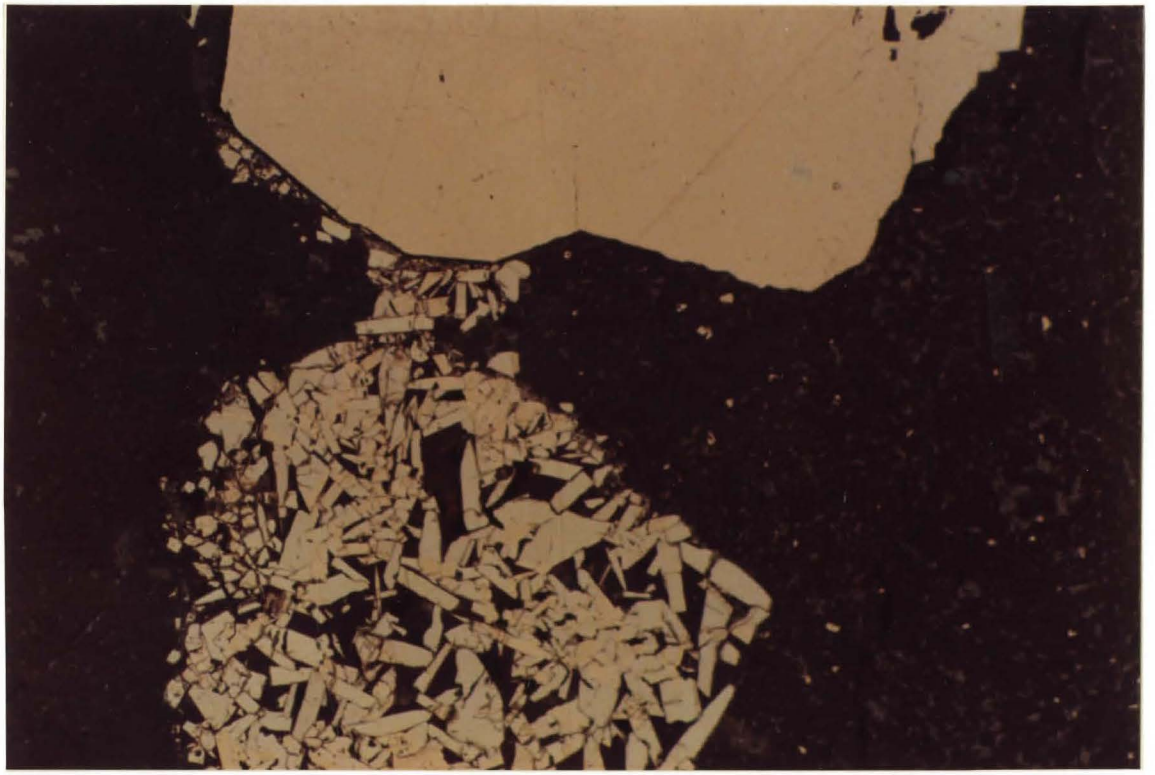

Plate 29: Cataclastic pyrite (p) showing sub-graining.Sphalerite (s) and chalco-pyrite (c) also seen. Colours not accurate. PPL. Field of view 1.5 mm.

Plate 30: Sphalerite (s) replacing pyrite along fractures. Note banding in sphalerite. PPL. Pyrite grain diameter 1 mm.

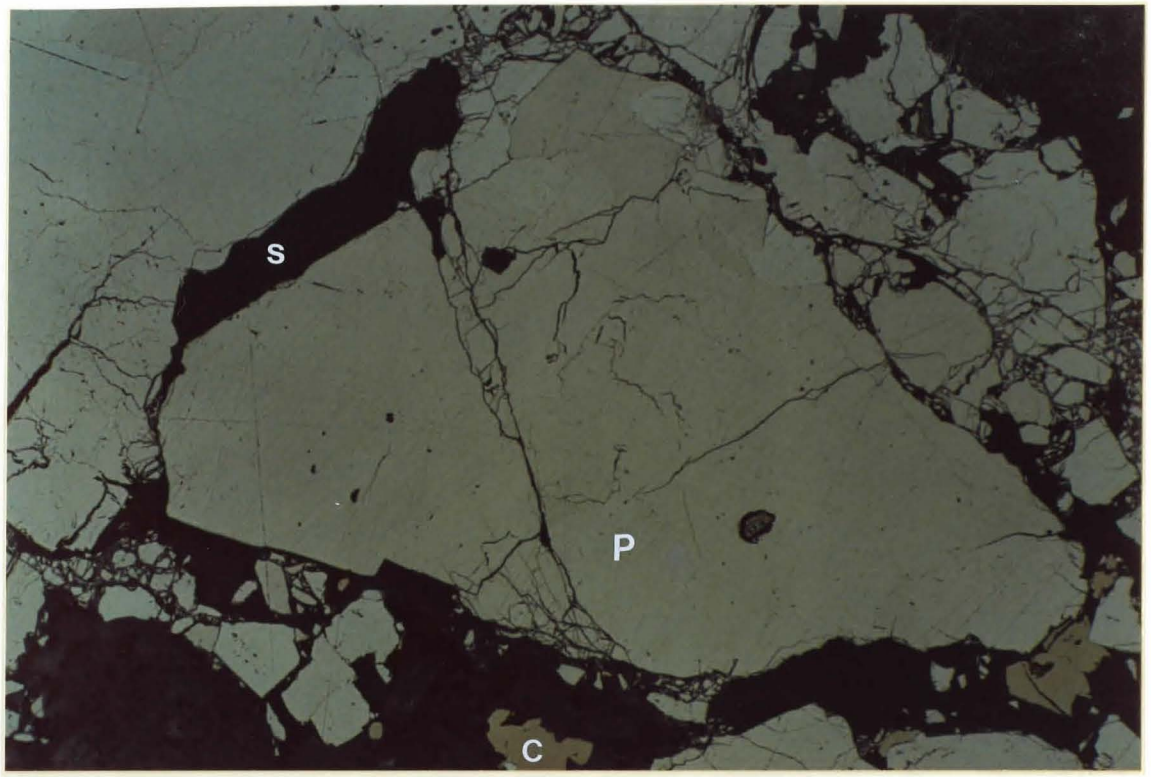
S
P
C

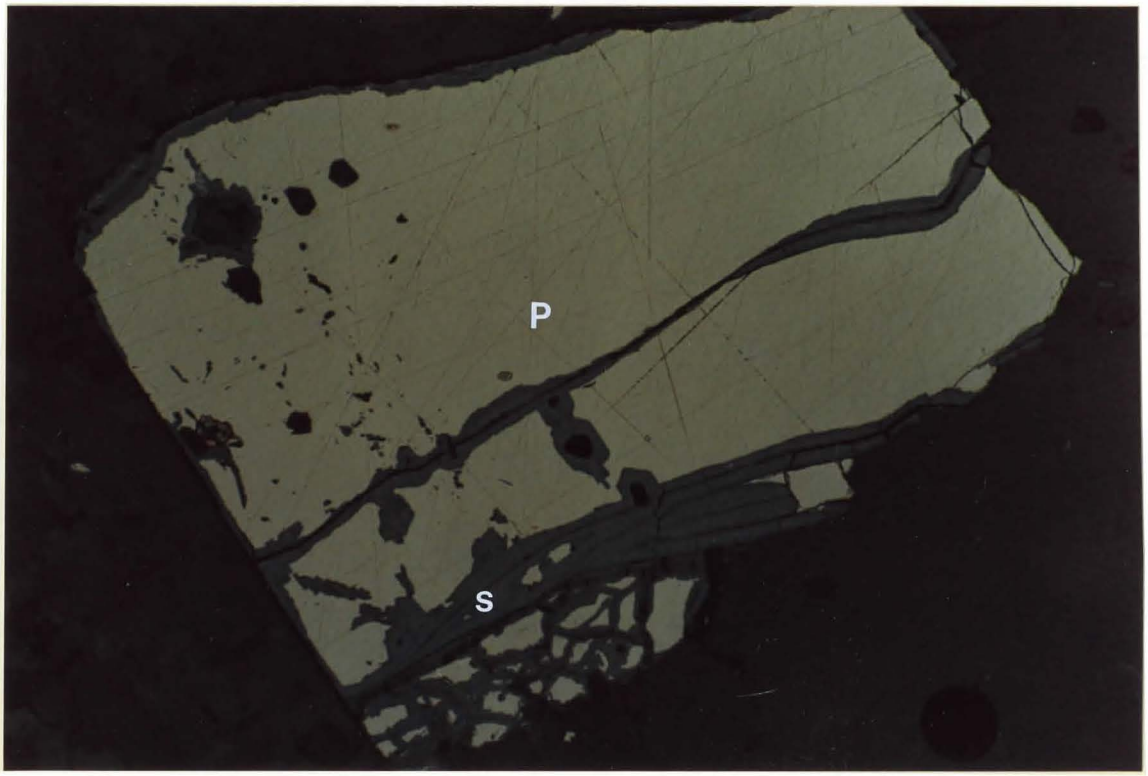
P
S

Plate 31: Highly anisotropic arsenopyrite (a) (purple/brown) blades intergrown with pyrite. Slightly crossed polars. Field of view 1 mm.

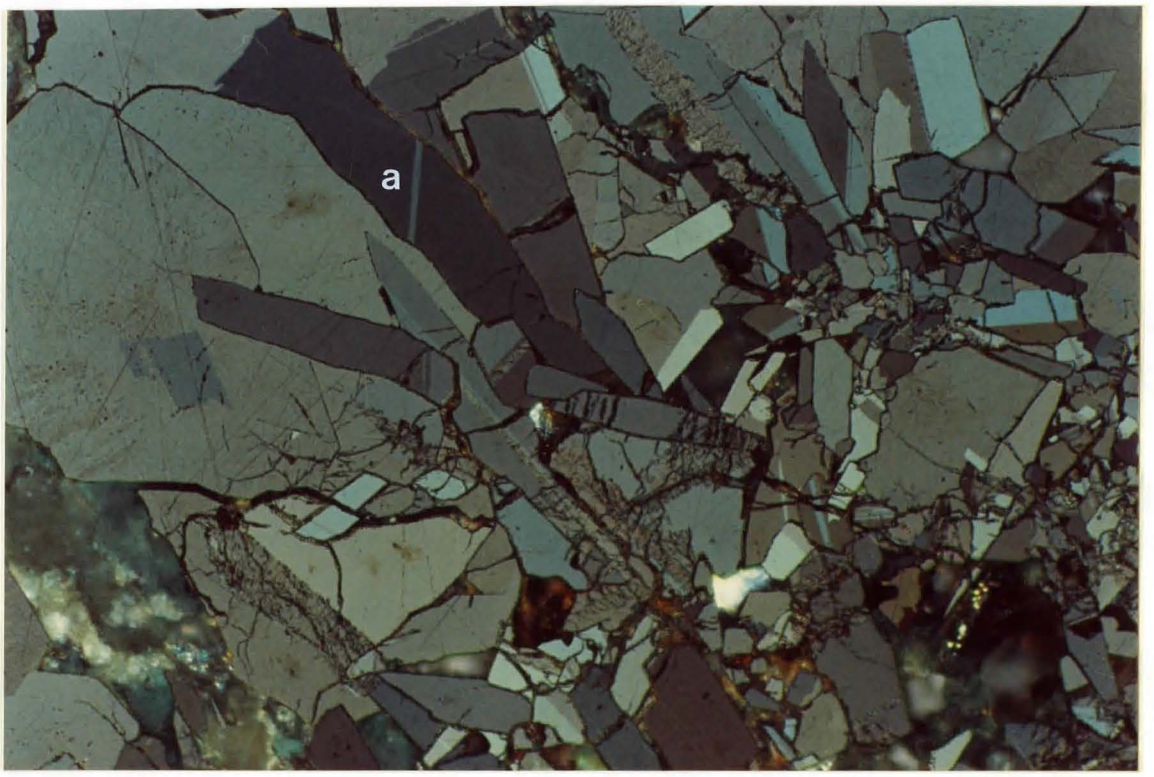
a

deformation (Stanton 1972). Cataclastic deformation and subgraining in the pyrite is evident in all slides (plate 26). Large idioblastic crystals of pyrite are seen in close proximity to small masses of euhedral tabular pyrite, possibly indicating recrystallization (plates 27,28).

Sphalerite is present in minor amounts and is found replacing pyrite (plate 30). Arsenopyrite is present as distinct blades intergrown with cataclastic pyrite (plate 31).

3.4 SEM Petrography

All SEM work was done on the ISI-DS-130 SEM housed in the Life Sciences department at McMaster University. The Princeton Gamma Tech (PGT) Energy Dispersive X-ray system (EDX) electron microprobe was used in an attempt to qualitatively identify the albite content of plagioclase feldspars and the Fe-Mg content of chlorite. Even semi-quantitative information is very difficult to

determine with any degree of certainty using this instrument as it has not yet been calibrated against a set of well defined mineral standards.

The peaks of the EDX spectra are identified using the PGT computer, the relative elemental abundances can be compared with the crystal morphology and an attempt to identify the mineral can then be made. Crystal morphology is often the primary method of identification. Minerals such as plagioclase have very distinct morphologies and are thus quickly and easily identified. Correlation of the peak heights of Al, Si, K and Ca are roughly proportional to their concentrations however, problems occur when comparing peak heights to concentration for both low- and high-atomic number elements (Welton 1984).

Na is the lightest element (Z=11) which can be detected using EDX analysis. An addition problem is that the peak heights for low-atomic number elements such as Na and Mg are always reduced relative to their concentration due to absorption of their low-energy X-rays by the Be window of the dectector (Welton 1984). Therefore the amount of Na relative to Ca will be

consistently underestimated in minerals such as plagioclase.

Carbon coated, polished thin sections were used for the EDX analysis and Au sputter coated chip samples (approximately 2 cm in diameter) were used for secondary image SEM micrographs. The scale bars on all micrographs are accurate, the magnification, however, is not.

Plate 32 is an SEM micrograph of a sample of the severly altered suite. Delicate quench textures are emphasized in this photograph. The EDX spectrum (figure2) for the central swallow-tailed microlite in this micrograph indicates a total absence of Ca and a distinct Na peak. As disscussed previously the abundance of Na relative to Ca is consistently underestimated in EDX analysis and therefore this spectrum is taken as very strong evidence that the plagioclase present is albite.

Plate 33 is a SEM micrograph of two plagioclase phenocrysts of the 'fresh' suite. The plagioclase can be identified on the basis of its morphology as can the

Plate 32: Backscatter image of plagioclase microlites of the severely altered suite. Note swallow tails with aspect ratios up to 25:1 (centre), belt buckle microlites (upper right), sheath spherulites (right centre). Field of view approximately 1750 microns.

Figure 2: EDX spectrum - distinct Na peak, absence of Ca peak is strong evidence that these microlites are albite.

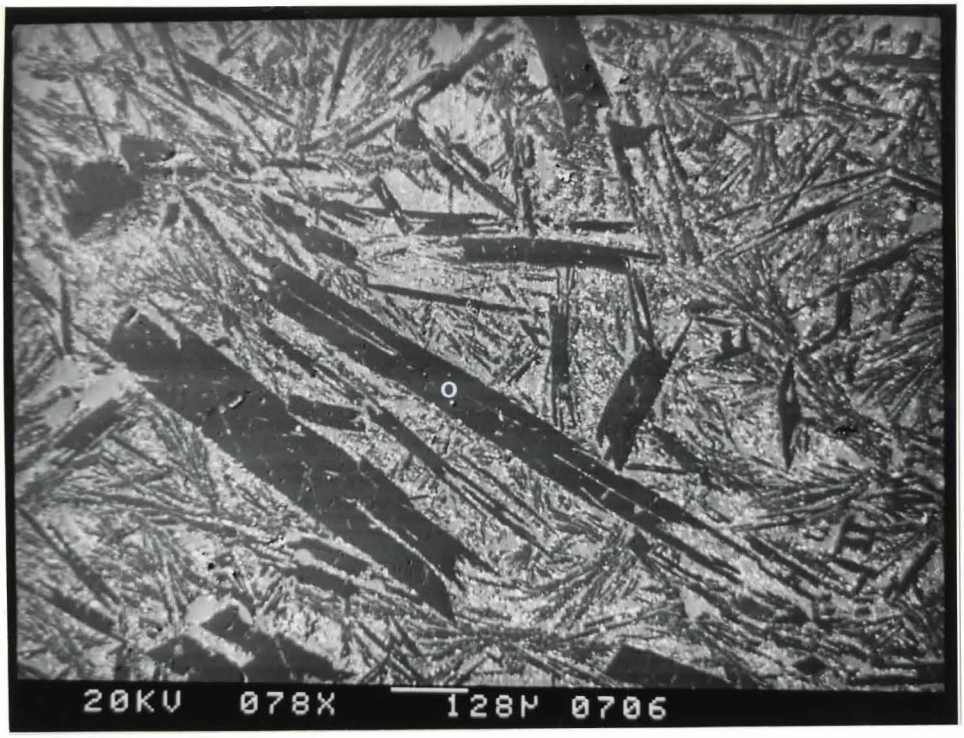

PLAGIOCLASE - ALBITE

SPECTRUM LABEL

13-PLAG

SPECTRUM FILE NAME

5S

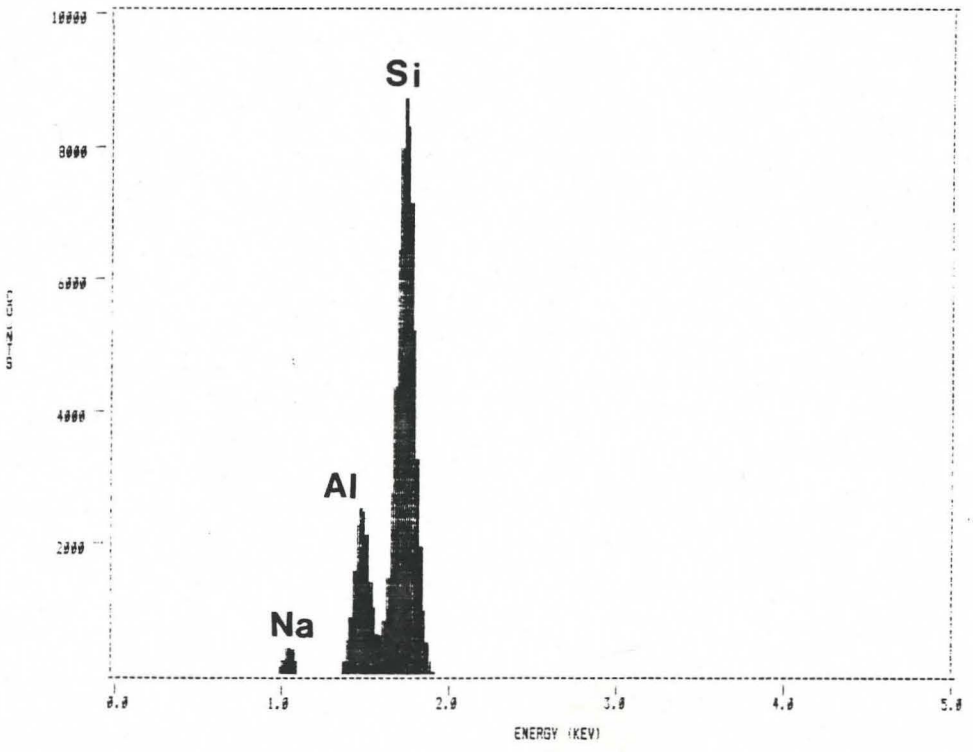

PIGITI

Plate 33: Fresh suite. Backscatter image of two large plagioclase phenocrysts showing considerable degradation. Fine white flakes surrounding the plagioclase are Fe-rich chlorite. High relief, white mineral between plagioclase laths is likely sphene. Field of view approximately 425 microns.

Figure 3: EDX spectrum of plagioclase. Note approximately equal Ca and Na peaks.

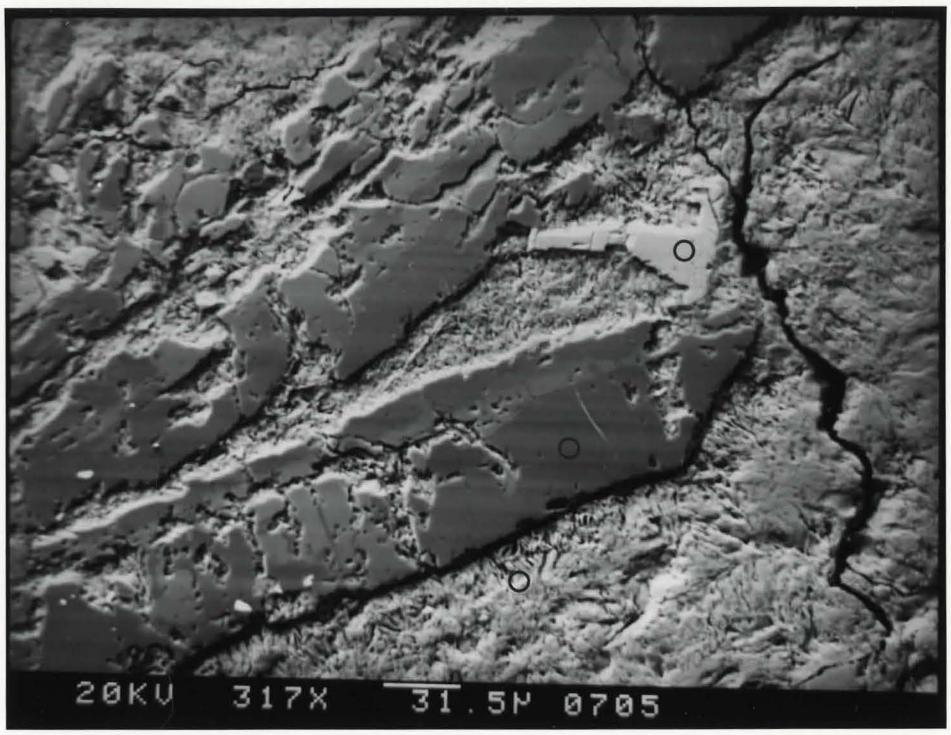

PLAGIOCLASE

SPECTRUM LABEL

12-PLAG-DARK AREA

SPECTRUM FILE NAME

3S

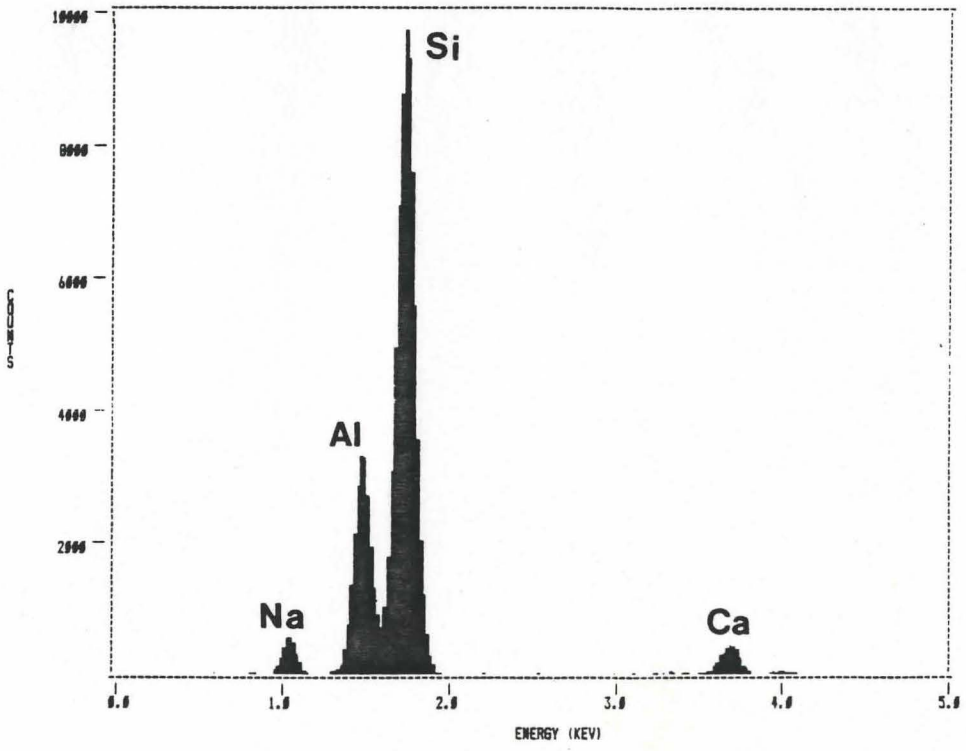

PIGITI

Figure 4: EDX spectrum of Fe-rich chlorite. Spectrum indicates the major elements Si, Al, Mg and Fe. Here the elemental EDX analysis is very important, otherwise this chlorite might be confused with other rosette-like minerals (Welton 1984)

Figure 5: EDX spectrum of sphene. Large peaks of Si, Ca and Ti indicate that this mineral is sphene ($CaTiO_5$).

CHLORITE

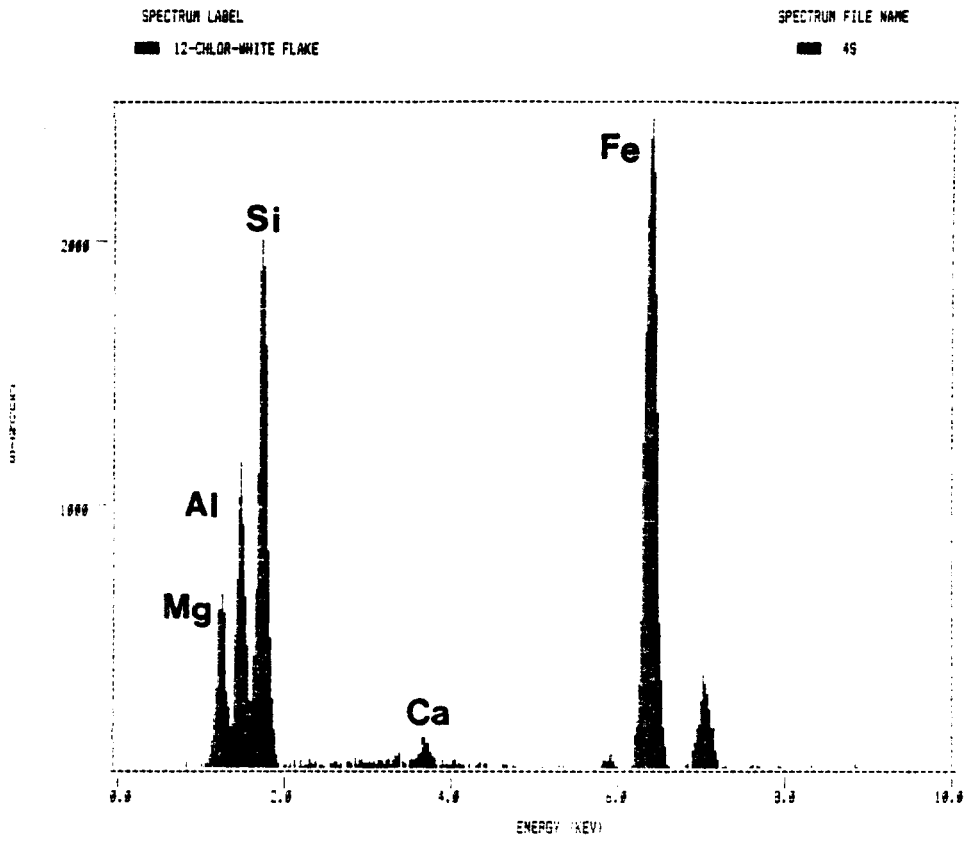

PIGITI

SPHENE

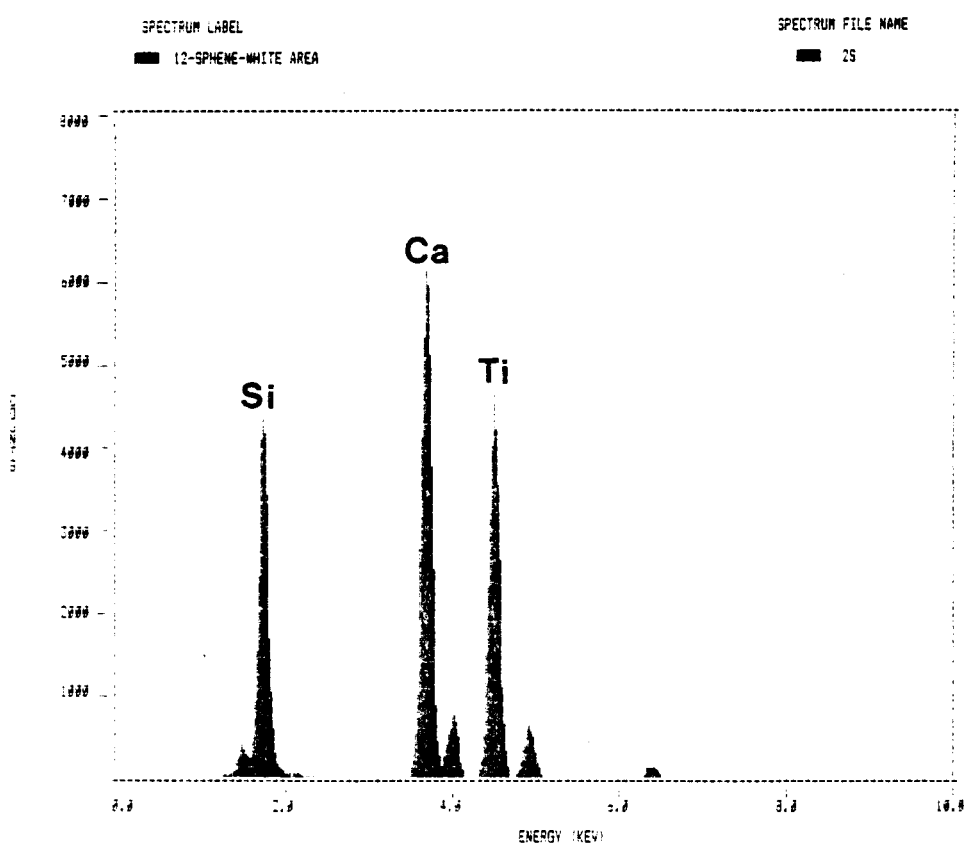

intersertal chlorite (white flakes) that surround the plagioclase. Sphene however, was identified by its Ca and Ti peaks on the EDX spectrum (figure 5). The plagioclase spectrum (figure 3) for the 'fresh' suite shows approximately equal Na and Ca peaks. This is precisely what would be expected since the 'fresh' suite has not undergone the Ca depletion due to spilitization that has occured in the more altered suites. Thus, in this instance, the EDX analysis can be used to substantiate what has been shown by the petrography and major element geochemistry.

EDX analysis of the chlorite (figure 4) of this suite shows it to be relatively Fe-rich. Sphene appears as an irregularly shaped, high-relief, white mineral in plate 33. Identifcation was not possible using crystal morphology, however, the EDX spectrum (figure 5) shows distinct Si, Ca and Ti peaks. In all likelihood this mineral is sphene ($CaTiSiO_5$).

The presence of chlorite as a vesicle lining mineral was confirmed using the electron microprobe. Plate 34 shows a circular, partially filled vesicle set

Plate 34: Backscatter image of a circular, partially filled vesicle. Note the quench morphologies of the surrounding plagioclase microlites. The centre of the vesicle is empty, cracks seen are in resin. Light gray material rimming the vesicle is chlorite and bright white material is pyrite. Field of view approximately 1750 microns.

Figure 6: EDX spectrum of vesicle rim chlorite.

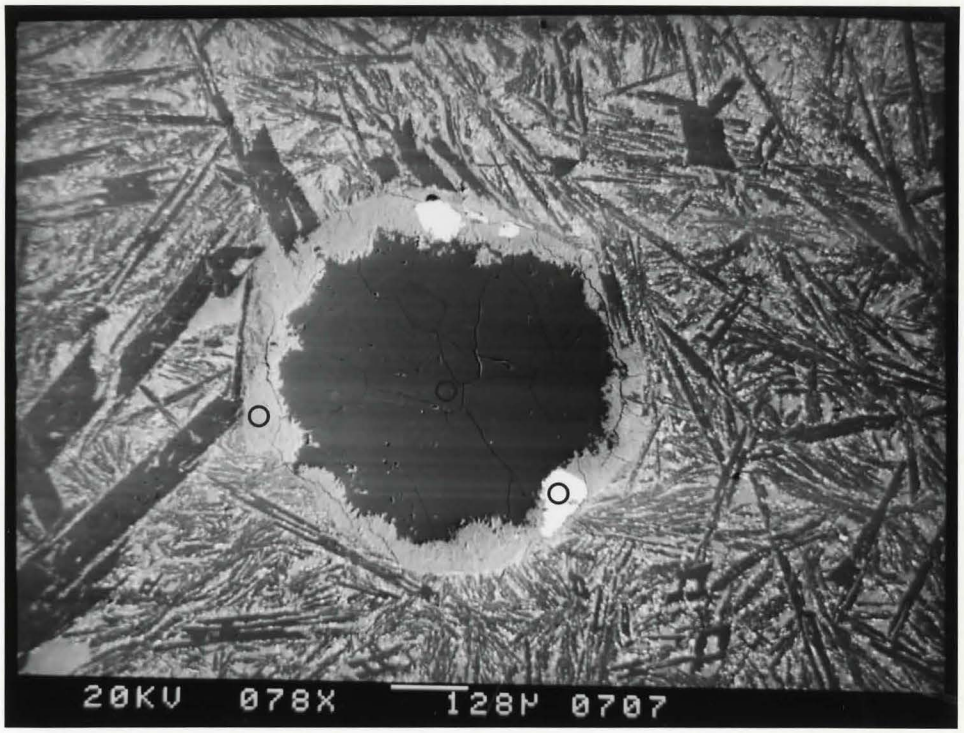

VESICLE RIM - CHLORITE

SPECTRUM LABEL

13-VESICLE RIM

SPECTRUM FILE NAME

7S

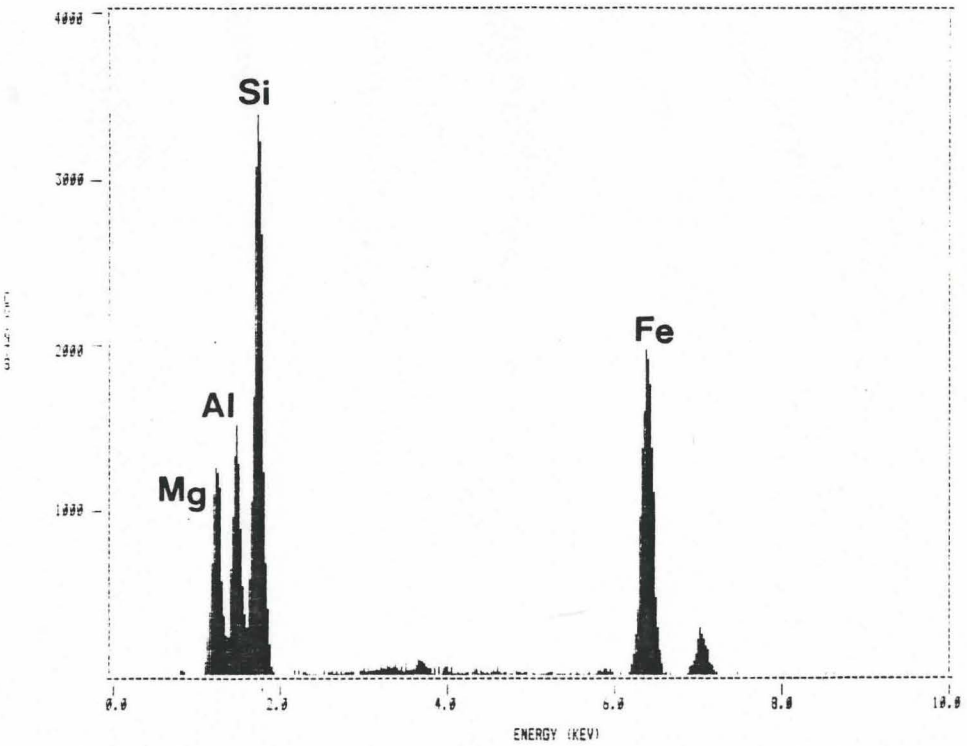

PIGITI

Figure 7: EDX spectrum of pyrite enclosed in chloritic rim of vesicle.

Figure 8: EDX spectrum of vesicle core. Single Si peak is that of the underlying glass slide.

PYRITE IN VESICLE RIM

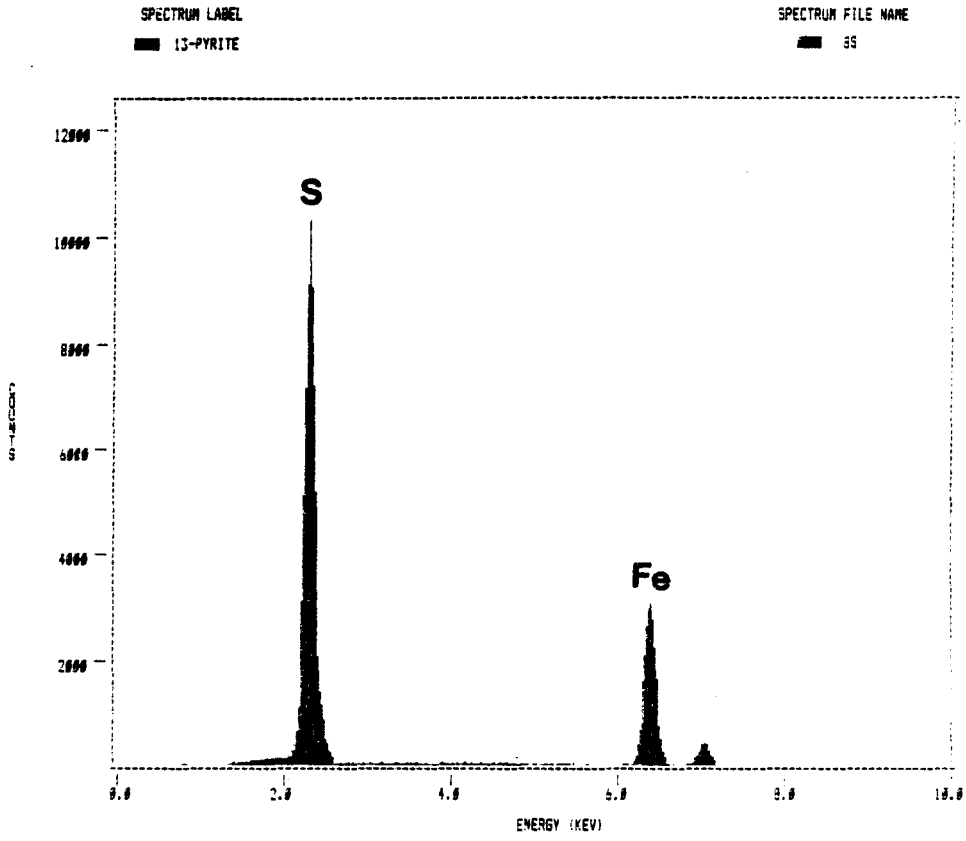

PIGITI

VESICLE CORE - VOID

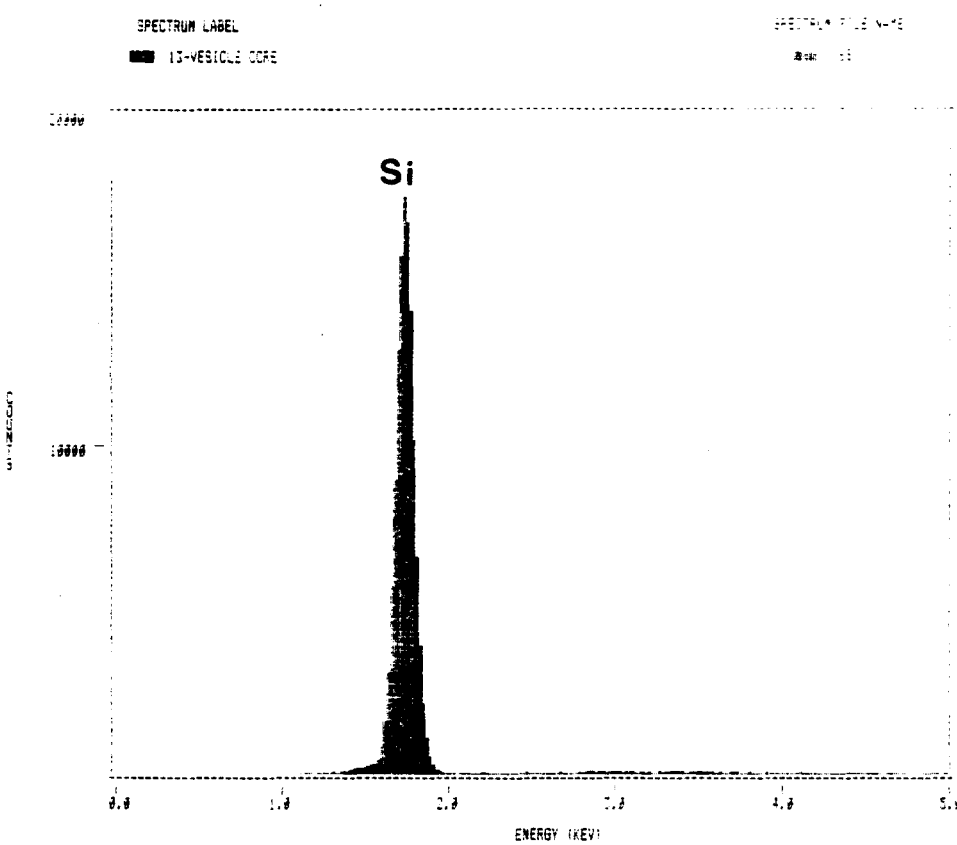

in a groundmass of plagioclase microlites. The core, rim and opaques of this vesicle were probed. The EDX spectrum (figure 6) of the rim shows the mineral present to be Fe-rich chlorite. The opaque mineral set in the chlorite is pyrite (figure 7). The centre of the vesicle is a void as evidenced by the single Si peak (due to the underlying glass slide) in figure 8. If the core of this vesicle were basaltic glass one would expect to see several other major element peaks such as Al, Ca, Na, Fe etc. due to impurities and noncrystalline phases, on the EDX spectrum.

The microprobe was also used to confirm the composition of the highly anisotropic ore mineral shown in plate 28. Microhardness tests could not be done due to the very small grain size of this mineral. However, the EDX spectrum (figure 9) shows large Fe and S peaks and no As peak. Therefore arsenopyrite (FeAsS) can be ruled out and it can be said that the recrystalling ore mineral seen in plates 28 and 35 is pyrite.

Chip samples were also examined using secondary imaging. Pyrite (plate 36), authigenic clays and gypsum (plate 37) were identified based solely on their crystal morphology.

Plate 35: An enlarged view of recrystallizing pyrite shown in plate 28. Back-scatter image. Field of view approximately 375 microns.

Figure 9: EDX spectrum of above pyrite. Prominent Fe and S peaks and absence of an As peak indicate that the ore mineral seen in plate 28 is indeed anisotropic pyrite (FeS_2) and not arseno-pyrite (FeAsS).

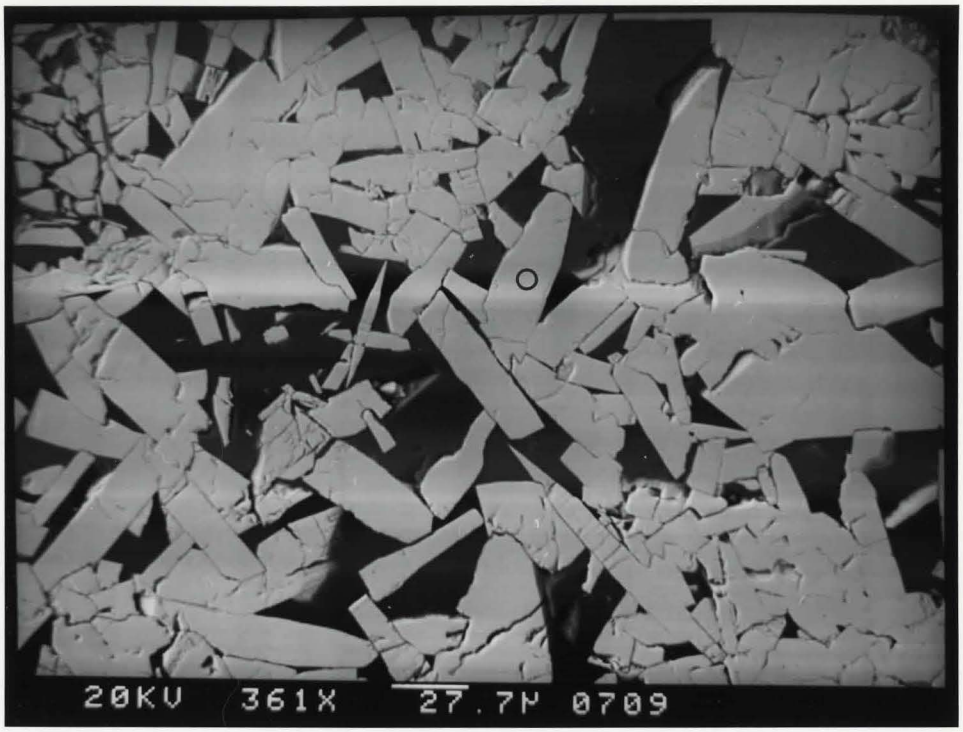

PYRITE

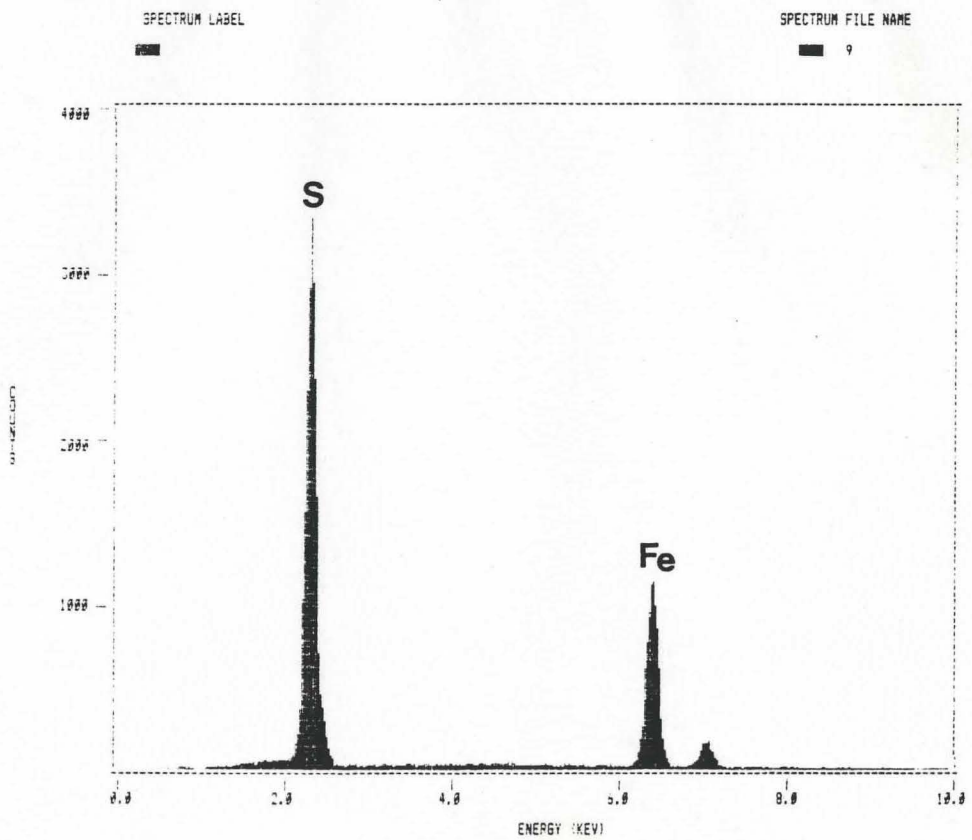

PIGITI

Plate 36: Aggregates of well developed euhedral cubic pyrite with authigenic clay overgrowths (?). Note large pyritohedron in left background. Secondary image. Field of view approx. 450 microns.

Plate 37: Gypsum (?) rosettes. Short prismatic laths arranged into a rosette. Secondary image. Field of view approx. 525 microns.

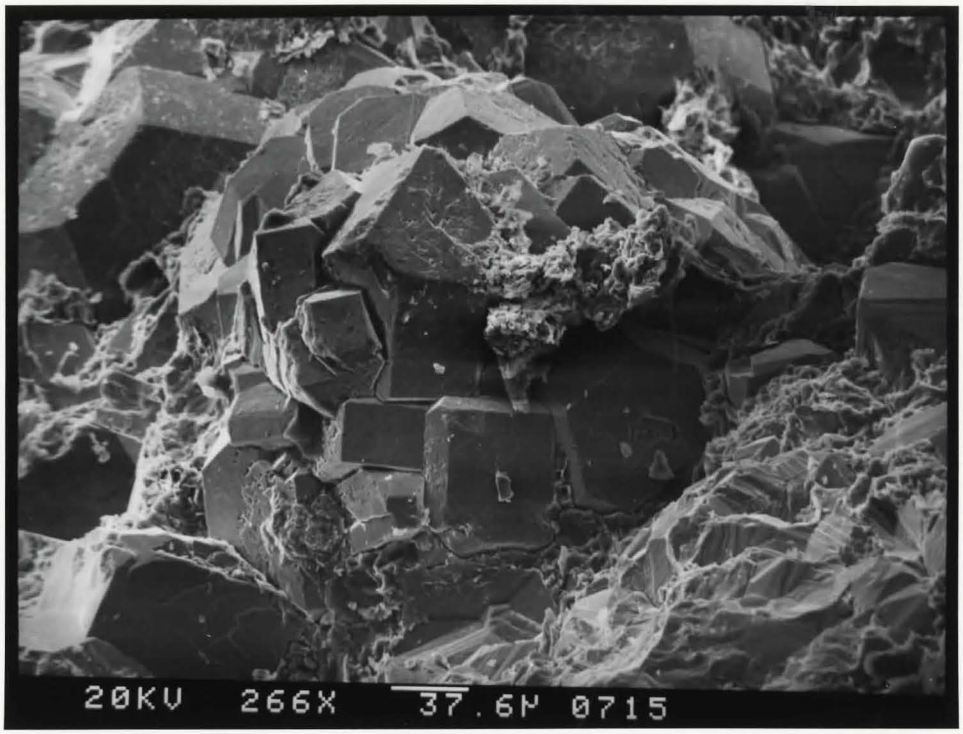
20KV 266X 37.6µ 0715


20KV 261X 38.3µ 0713

CHAPTER FOUR

GEOCHEMISTRY

4.1 Analytical Procedure

In selecting samples for analysis, care was taken to remove all weathered surfaces prior to crushing. Representative, fresh portions of the samples were initially crushed in a Chipmunk jaw crusher. The samples were then ground in a ceramic disc pulverizer and powdered in a Spex Industries tungsten-carbide ring shatterbox to -200 mesh.

4.1.1 X-ray Fluorescence Analysis

Major and trace element analyses were carried out using a Phillips, Model 1450 AHP automatic sequential x-ray fluorescene spectrometer housed in the Department of Geology, McMaster University. Raw data were corrected for absorption and enhancement effects according to the method outlined by Marchand (1973) and final values were determined using USGS rock standards: NIM-G, NIM-N,

BR, JG-1, SY-2, SY-3, BCR-1, AGV-1, NIM-P, MRG-1, STM-1, G-2, JB-1, W-1 and GSP-1.

4.1.1.1 Major Elements

The glass pellets used for major element analysis were prepared by fusing a mixture of 0.5000 grams of sample and 3.0000 grams of a 50:50 mixture of lithium tetraborate:lithium metaborate flux in a platinum crucible. The sulfide content of many samples prevented the preparation of such fusions due to the destructive nature of the sulfides on the platinum crucible. Therefore all samples were analyzed using pressed powder pellets and these values were compared to the available data on fusions. The agreement was found to be good for all major elements with the exception of sodium. Differences as high as 100% were seen between Na values determined on fusions and powder pellets. Variable results were also common for values determined on duplicate powder pellets.

An attempt was made to substantiate the precision of the Na_2O values determined by XRF using atomic absorption spectroscopy. Once again the results were

ambiguous. No consistent pattern was seen. Some values determined by XRF had underestimated the Na_2O content by up to 25% while others were 20% too high, relative to those values found using atomic absorption.

Only a rigorous comparison of Na_2O values determined by XRF (on powder pellets and fusions) to those determined by atomic absorption spectroscopy will clarify the situation. Due to the difficultly of achieving reproducible results for Na_2O values by the method XRF, the future use of atomic absorption is recommended. However, due to the small sample size (five) analyzed by atomic absorption, and the ambiguity of those results, the author has listed the Na_2O values determined for powder pellets by XRF in Table 1.

The oxides analyzed for were: SiO_2 , Al_2O_3 , Fe_2O_3 total, MgO, CaO, Na_2O, K_2O, TiO_2 , MnO and P_2O_5 . A Cr - X ray tube was used throughout.

4.1.1.2 Trace Elements

Pressed powder pellets were prepared by mixing approximately 3 grams of sample with 4-5 drops of

'Mowiol', a polyvinyl alcohol binder. This mixture was then placed in an aluminum disc and compacted in a hydraulic press under 20 tons of pressure for 3 minutes. The trace elements analyzed for were: Rb, Sr, Y, Zr, Nb, As, Zn, Ni,Co, Cr, V, Cu and Pb.

4.1.2 Determination of Volatiles

The total volatile content of all samples was determined using Loss on Ignition (L.O.I.). Sample powders weighing approximately 4-7 grams were accurately weighed (to 4 decimal places) and transfered into clean, pre-weighed porcelain crucibles. The crucibles were then heated for two hours at 1050°C. The samples were removed from the oven, allowed to cool, reweighed and the loss of weight determined. The procedure was then repeated with a smaller sample size (approximately 1 gram) with one hour heating and the results were averaged. The results of the two runs were found to be in excellent agreement, with less than a 5% difference found in all cases. The possible formation of a crust, resulting in nonhomogeneous heating, as well as oxidation of pyrite during the 2 hours of heating were, therefore, found not to be significant factors in the larger samples.

4.1.3 Sulfur Determination

The sulfur content of several samples was determined initially by XRF on powder pellets. These same samples and standards were then analyzed for S using the LECO WR-12 gas analyzer and a simple starch/iodide titration. A comparison of the LECO and XRF values showed the agreement to be consistently poor. Both high and low sulphur content samples showed variation of up to 35%.

It is the opinion of the author that the combustion/oxidation process and sensitive iodide titration method, used in LECO gas analysis, would yield far more reliable results than those of XRF.

4.1.4 Normative Mineral Calculations

CIPW norms were calculated using a computer programme by Mattison (1973). A conversion factor of

$$\% Fe_2O_3 = \% TiO_2 + 1.5$$

was used to derive FeO from Fe_2O_3 total. The results of these CIPW norm calculations are included in Table 2.

4.2 Results

The results of XRF analyses for the major and trace elements are listed in Table 1. The thesis samples show an enrichment in SiO_2, Na_2O, K_2O, P_2O_5 and H_2O relative to fresh mid-ocean ridge basalts (Melson et al.1968). Al_2O_3 and Fe_2O_3 values are variable but not outside the spectrum of oceanic tholeiites. Na_2O and CaO show the greatest deviation from the values of fresh mid-ocean ridge basalts. The range of Na_2O values for average, unaltered ocean floor basalts is 2.58 to 3.01 (average 2.70) and that of CaO is 10.46 to 11.51 (average 11.69) (Melson et al. 1968). The thesis samples show a depletion in CaO and a strong enrichment in Na_2O. There is a correspondence of high CaO values with low Na_2O values and vice versa (sample 21: CaO=0.80, Na_2O=5.85 and sample 12: CaO=9.58, Na_2O=3.15). All samples have significantly higher H_2O contents than unaltered mid-ocean ridge basalts (4.70-6.90 vs 0.93).

The trace element values of these samples are consistent with those outlined by Kay and Hubbard (1978).

	5	6	7	12	13	14	18	21	22	23	26
SiO_2	58.04	64.95	54.74	48.99	53.12	53.52	53.71	65.84	62.76	56.94	58.98
Al_2O_3	15.50	14.18	17.28	16.44	17.13	15.27	15.22	16.17	16.13	13.64	12.64
Fe_2O_3*	10.85	9.19	14.33	11.84	9.90	14.92	14.54	6.98	7.74	11.16	11.25
MgO	4.98	1.70	1.69	7.85	5.05	5.68	6.30	2.38	2.60	7.18	5.27
CaO	2.10	1.92	2.31	9.58	6.28	2.29	1.65	0.80	1.45	4.49	5.89
Na_2O	5.77	5.78	7.88	3.15	6.51	5.88	6.31	5.85	7.06	4.80	4.17
K_2O	0.29	0.17	0.26	0.42	0.20	0.47	0.29	0.44	0.45	0.16	0.25
TiO_2	2.12	1.83	1.34	1.37	1.49	1.59	1.56	1.36	1.57	1.33	1.24
MnO	0.13	0.08	0.04	0.24	0.14	0.16	0.17	0.04	0.05	0.18	0.18
P_2O_5	0.23	0.19	0.14	0.12	0.17	0.22	0.26	0.13	0.18	0.11	0.13
L.O.I	4.80	4.70	6.60	6.90	4.30	5.90	6.00	4.70	5.00	5.00	5.00
Rb	3	3	3	3	3	5	3	3	3	3	3
Sr	185	144	157	196	85	161	150	173	174	129	74
Y	33	27	16	24	25	18	23	21	22	28	28
Zr	152	139	104	111	121	123	128	119	140	103	101
Nb	10	7	7	8	12	5	7	9	11	7	10
As	18	29	26	2	20	3	22	101	91	21	2
Zn	90	55	59	87	59	133	108	35	41	118	159
Ni	51	44	74	102	76	54	67	39	35	52	51
Co	101	83	53	53	70	65	69	59	144	79	48
Cr	183	113	379	363	366	167	172	242	178	184	190
V	404	334	232	224	229	325	322	358	348	305	262
Cu	88	155	-	47	55	63	53	144	138	72	46
Pb	14	14	18	11	8	17	14	9	16	10	8

TABLE 1: Major and trace element analysis.

* total Fe calculated as Fe_2O_3

all data normalized to 100% - volatile free

C.I.P.W NORMS

	5	6	7	12	13	14	18	21	22	23	26
Q	8.50	21.60	-	28.40	-	-	-	23.00	11.00	5.00	12.00
Or	1.70	1.00	1.50	2.50	1.20	2.80	1.70	2.60	2.70	0.90	1.50
Ab	48.80	48.90	65.00	1.30	49.30	49.70	53.40	49.50	59.70	40.60	35.30
An	8.90	8.20	10.50	2.00	16.90	9.90	6.40	3.10	6.00	15.20	15.00
Ne	-	-	0.90	-	3.10	-	-	-	-	-	-
Di	-	-	-	-	10.60	-	-	-	-	5.10	10.90
Hy	20.40	10.90	-	31.60	-	22.80	20.60	11.00	12.00	25.10	17.70
Ol	-	-	12.80	-	11.30	3.30	5.80	-	-	-	-
Cor	2.50	1.50	0.20	15.00	-	1.50	2.20	5.00	6.00	-	-
Mt	4.70	4.00	6.20	5.20	4.30	6.50	6.30	3.00	3.40	4.90	4.90
Il	4.00	3.50	2.50	0.70	2.80	3.00	3.00	2.60	3.00	2.50	2.40
Ap	0.50	0.40	0.30	0.30	0.40	0.50	0.60	0.30	0.40	0.30	0.30

TABLE 2: Calculated CIPW norms

CHAPTER FIVE

DISCUSSION

5.1 Petrography

The assemblage chlorite, albite, epidote/clinozoisite, calcite is diagnostic of the greenschist facies of low grade metamorphism (Winkler 1979). These minerals are ubiquitous in all samples. This same paragenetic assemblage is recognized in the lower pillow lava unit at Blow-Me-Down Mountain and in other ophiolite suites. Einarson (1975) has identified a depth controlled sequence of metamorphic facies that appear to represent ocean-floor type burial metamorphism occuring in an environment of high geothermal gradient. The pillow lava unit of Blow-Me-Down mountain exhibits a downward progression from very low grade prenhite-pumpellyite facies to low grade greenschist facies metamorphism. The boundary between the two zones coincides with the lithic subdivision between the upper and lower pillow lava sequences (Einarson 1975).

The distribution and grade of metamorphism is controlled by circulating sea water and the thermal gradient. Due to the impervious nature of the gabbros,

the effects of hydrothermal alteration are usually restricted to the pillow lavas and sheeted dike complex of ophiolites (Gass and Smewing 1973). The downward progression from zeolite to greenschist, and even amphibolite facies in the upper parts of the layered gabbros, is a common feature of many ophiolite complexes (Spooner and Fyfe 1973).

The complete degradation of primary mineralogy with the preservation of the original igneous textures is characteristic of thermally metamorphosed ophiolitic basalts. The presence of primary textures in altered basalts was the basis of the arguement that spilites are crystallized from primary spilitic magmas (Amstutz 1974). It is now widely accepted however, that spilites are the result of low grade thermal metamorphic alteration of ordinary tholeiitic basalts by hot, circulating sea water in the upper parts of newly-formed oceanic crust (Vallance 1973).

All thin sections examined show very good textual preservation. Intersertal texture, as well as the delicate quench crystal morphologies of plagioclase microlites were equally well preserved in all suites. For this reason, textual preservation was found not be an adequate criterion on which to base the relative

degree of alteration of these metabasalts.

The preservation of primary igneous minerals (olivine and clinopyroxene) and the presence and type of inclusions in the phenocrysts were found to be the most useful criteria for determining the degree of alteration in these rocks.

5.2 Geochemistry

The effects of submarine weathering and metamorphism on sea-floor basalts are well documented (Hart et al 1974, Spooner and Fyfe 1973). Basalt - sea water interaction leads to the conversion of fresh oceanic tholeiites to low grade metamorphosed basalts or spilites (Vallance 1974). Significant changes in the bulk chemistry of the basalts (both major and trace elements) results.

Several reactions occur between the primary anhydrous mineralogy of the freshly extruded, hot basalt and the surrounding sea water. Permeability has a significant influence on controlling the degree of alteration that occurs. Generally, the greater the water/rock ratio, the more extensive the alteration (Rona 1984).

The alteration of clinopyroxene and olivine to chlorite and clay minerals results in the loss of Si, Ca and Mg. The loss of Ca may be complete, owing to the high solubility of Ca^{2+} in sea water, particularily under conditionsof high partial pressure of CO_2. The Si content (by volume) of clinopyroxene is approximately 50% while that of chlorite is 25-30%. In this way the SiO_2 content of a basalt can decrease by up to 13% during spilitization (Muller and Strauss 1984). The liberated Si may travel upwards, carried by hot circulating brines, through the extensively fractured volcanic pile to precipitate at the surface. The alteration of calcic plagioclase to smectite will also liberate Ca and extract K from sea water to form illite (Hart et al. 1974).

The albitization of calcic plagioclase involves a net gain of Na and Si and a net loss of Ca and Al. This process of Na-metasomatism increases the Na_2O content of the spilitized basalt considerably. The palagonization of basaltic glass has been shown to be a source of Ca and Na for sea water and a sink for K and Fe (Moore 1966).

Ti and Al are considered by many authors (Hart 1970, Muller and Strauss 1984, Spooner and Fyfe 1973) to

be relatively immobile during submarine weathering. Al_2O_3 has however, been shown to be lost during hydrothermal alteration of basalts to the greenschist facies (Hart et al. 1974). An increase in water content is one consequenece of spilitization that is universally accepted.

Metasomatism and submarine metamorphism also alter the trace element concentration of basalts. Ba, Cu, Zn, Ni and Rb are especially susceptible to mobilization while Zr, Sr and V are more stable under these conditions. Cr, Co, Y and Nb are considered to be essentially immobile (Hart 1974, Muller and Strauss 1984).

Table 3 is a comparison of the thesis area rocks with unaltered volcanics of the lower pillow lava sequence at Blow-Me-Down Mountain (Duke and Hutchinson 1973) and fresh mid-ocean ridge basalts (Melson 1968). Several significant variations are seen. A lose of Ca and Mg, and a gain of K, P, Na, Si and H_2O relative to the fresh basalts has occurred. These trends parallel those seen in spilitized basalts, as described by Cann (1970).

	Fresh Mid-Oceanic Basalt (Melson et al. 1968)	Unaltered Lower Volcanics Blow-Me-Down Mountain (Duke and Hutchinson 1973)	Thesis Area Pillow Lavas (Sample Ranges)
SiO_2	49.74	46.65	48.99 - 65.84
Al_2O_3	16.52	16.24	12.64 - 17.28
Fe_2O_3*	9.25	10.18	6.98 - 14.92
MgO	7.41	9.80	1.69 - 7.85
CaO	11.69	9.38	0.80 - 9.85
Na_2O	2.70	3.21	3.15 - 7.88
K_2O	0.21	0.19	0.16 - 0.47
TiO_2	1.53	0.96	1.24 - 2.12
MnO	0.16	0.23	0.04 - 0.24
P_2O_5	0.06	0.15	0.11 - 0.26
L.O.I.	0.93	4.00	4.70 - 6.90

TABLE 3: Chemical analysis of pillow lavas from various areas.

* total Fe calculated as Fe_2O_3

The high mobility and resultant redistribution of total Fe, MgO and the alkalis (Na + K) leads to a wide scatter on an AFM diagram (figure 10). The AFM trends of the Bay of Islands, Lushs Bight and Mings Bight ophiolites of Newfoundland all show similar scatters across the tholeiite - calc-alkaline trend (Strong 1977).

The relative mobility of several of the major elements under the conditions of submarine metamorphism requires special caution when applying rock classification schemes based upon the relative abundance of these elements. Fyon (1980) has shown that for Mg-tholeiites with volatiles in excess of 4% that the application of the Jensen Cation Plot leads to diverse and incorrect classification. The wide data scatter seen on the total alkalis vs SiO_2 plot (figure11) is also the result of the mobility of Na, K, and SiO_2 during hydrothermal alteration.

Hughes (1973) has developed a plot based upon Na_2O and K_2O abundances that demonstrates the effect of metasomatic alteration on igneous rocks. The data points of figure 12 plot outside the 'igneous spectrum'

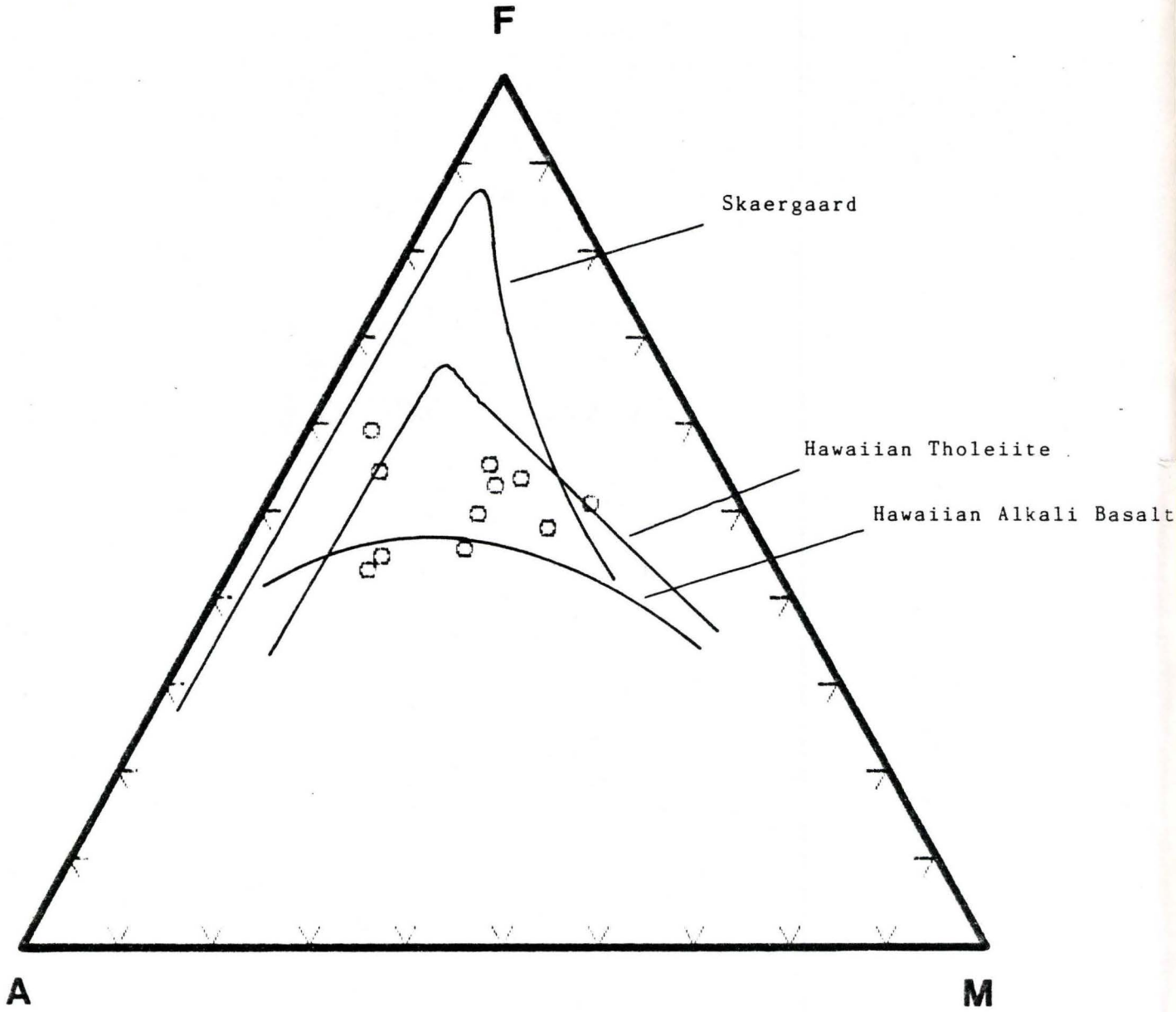

Figure10: AFM Plot (after Irvine and Baragar 1971)

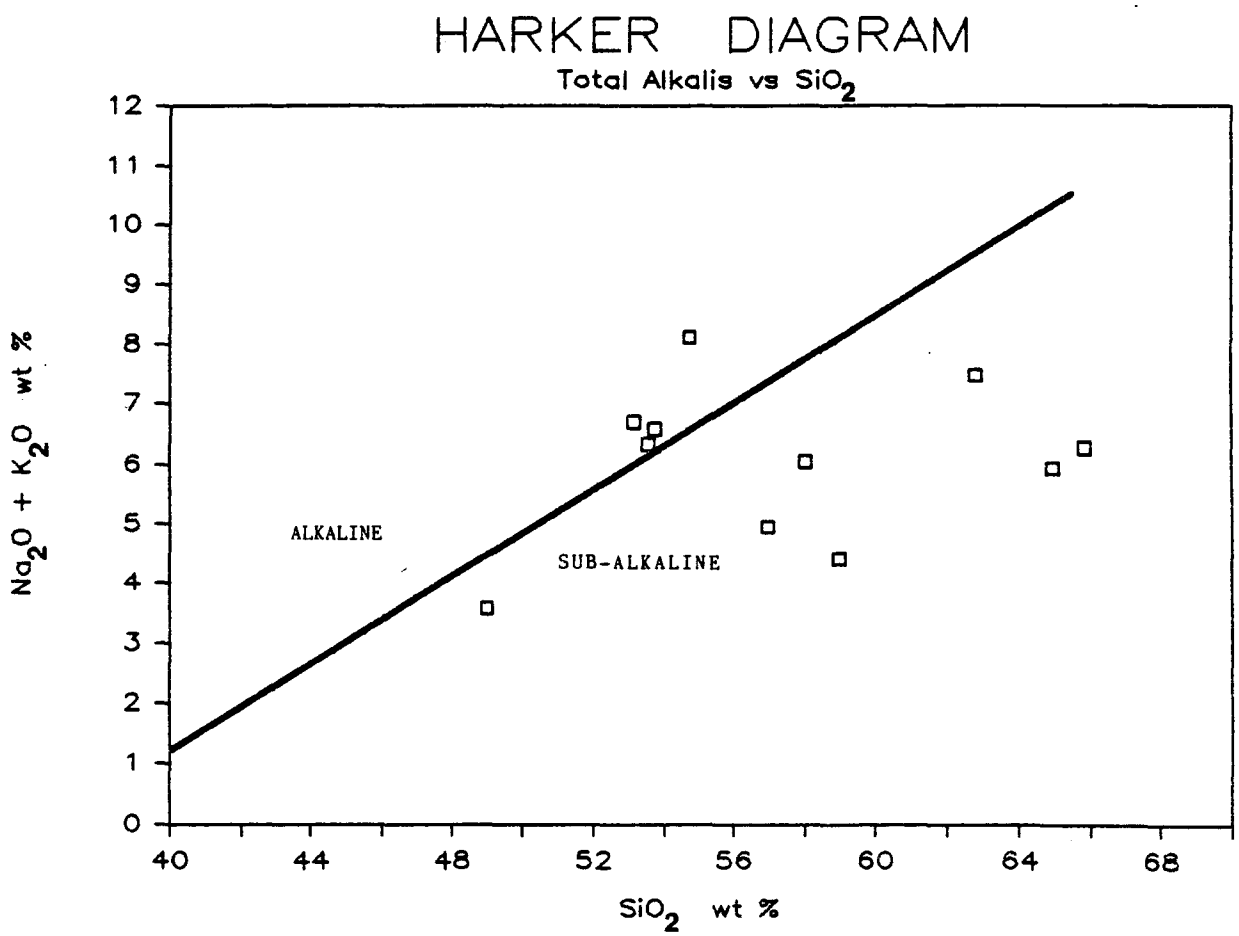

Figure 11: Total Alkalis vs SiO_2

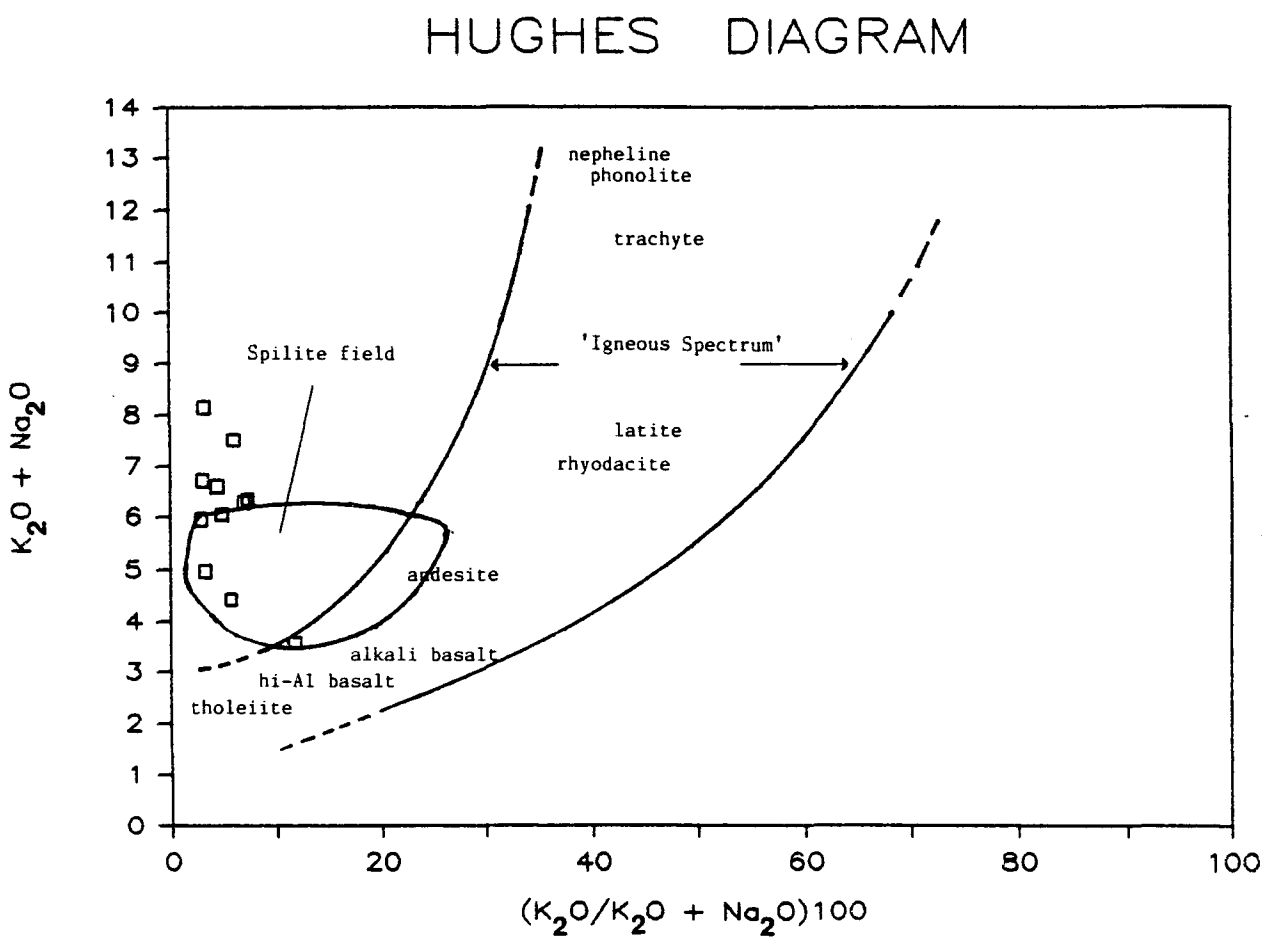

Figure 12 Hughes Diagram showing 'Igneous Spectrum' and Spilite Field (after Hughes 1973)

and therefore, according to Hughes, are metasomatic in nature. The effect of spilitization is to increase the Na content of the plagioclase (originally labradorite) which occupies approximately 55% by volume of the basalt. Therefore, during alteration, a vertical trend is developed from tholeiites to spilities as the Na_2O content of the basalt increases. Several data points in Figure 3 show Na-enrichment greater than that of the Virgin Islands samples used by Hughes to define the spilite field, and thus plot above this region.

The strong depletion of Mg in these rocks results in the scatter of points in Figure 13 . The samples plot in all fields except that of ocean ridge and floor. The effectiveness of the $MgO-FeO_T-Al_2O_3$ diagram in discriminating tectonic environments is greatly reduced by the effect of metasomatism on basalts and the tendency for hydrothermal alteration to make tholeiites appear geochemically similar to alkali basalts is apparent (Muller and Strauss 1984).

Immobile trace and major elements can be used to differentiate tholeiites from alkali basalts, as well as to identify the tectonic environment in which the basalts were emplaced. Winchester and Floyd (1976) have

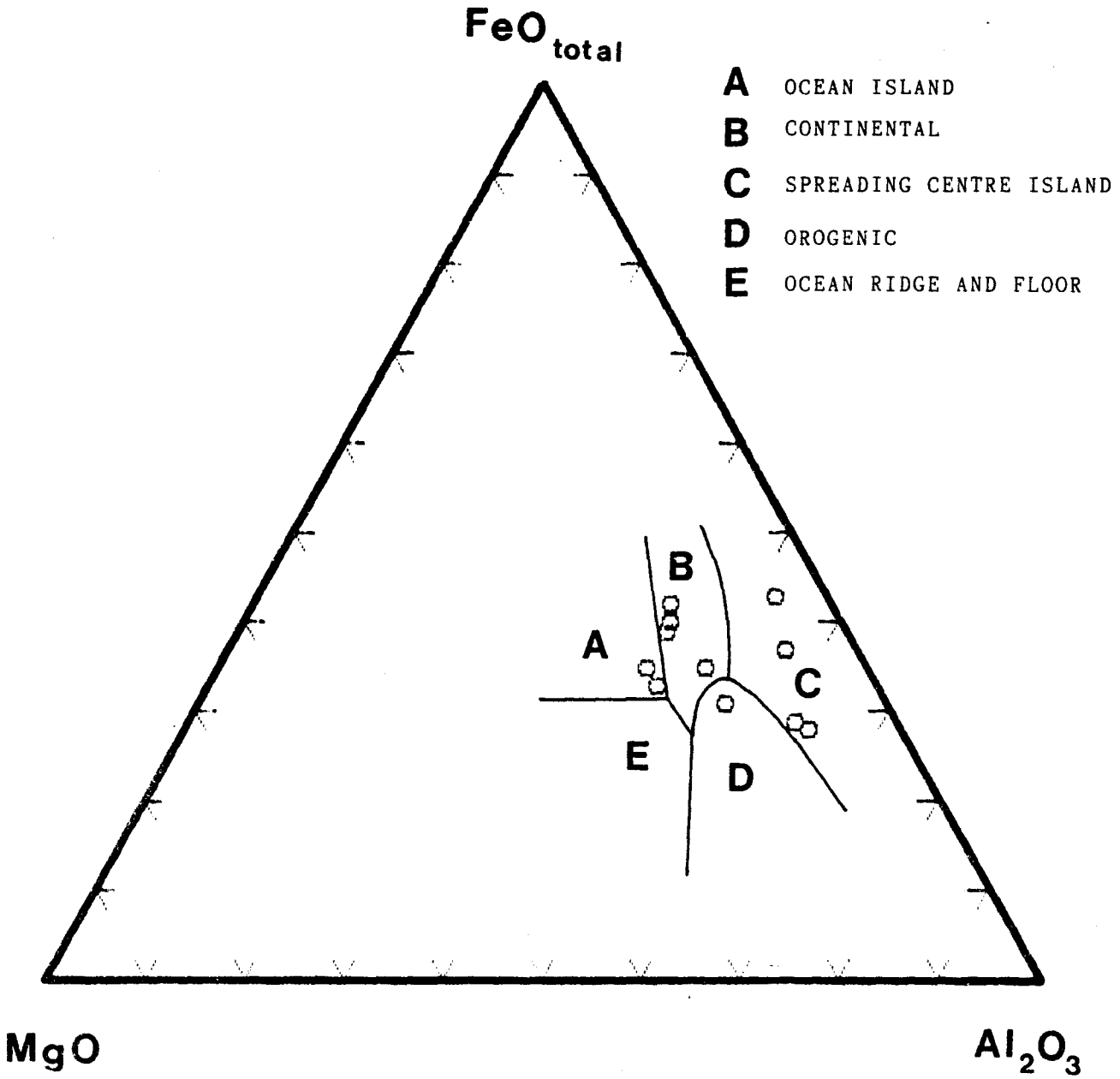

Figure13: MgO - FeO_T - Al_2O_3 Disriminant Diagram
(after Pearce, Gorman and Birkett 1977)

successfully used Ti, Zr, P, Y and Nb to identify the parentage of both fresh and altered basaltic rocks. It has been demonstrated by the authors that progressive hydration and spilitization of modern basalts has no effect on the Zr/P_2O_5 ratio. The tholeiitic affinity of the Bay of Islands has been demonstrated by Winchester and Floyd (1976) using TiO_2 - Y/Nb and TiO_2 - Zr/P_2O_5 diagrams. All data points of figure 14 are seen to fall within the oceanic tholeiite field of the Floyd-Winchester plots.

Based upon the stability of Ti, Zr, Y, Nb and Sr during submarine weathering and metamorphism, Pearce and Cann (1971) have successfully used discriminant analyses to identify tectonic environments of ophiolite origin. Caution must be used in the application of the Ti-Sr-Zr plot as Sr can be affected during greenschist facies metamorphism. Despite this fact, all data points are tightly clustered within the ocean floor basalt field of the forementioned plot (figure 15). In figure16, the majority of data points plot just within the oceanic island-continental basalt field, while only two samples fall within the ocean floor basalt field. The similar geochemical behaviour of Y and Ca could explain this trend. A strong Ca depletion is the result of

Figure 14a : TiO_2 vs Y/Nb diagram showing the oceanic tholeiite field. (after Floyd and Winchester 1975)

Figure 14b : Nb/Y vs Zr/P_2O_5 diagram showing the oceanic tholeiite field of Floyd and Winchester (1975)

FLOYD—WINCHESTER PLOT

TiO_2 – Y/Nb

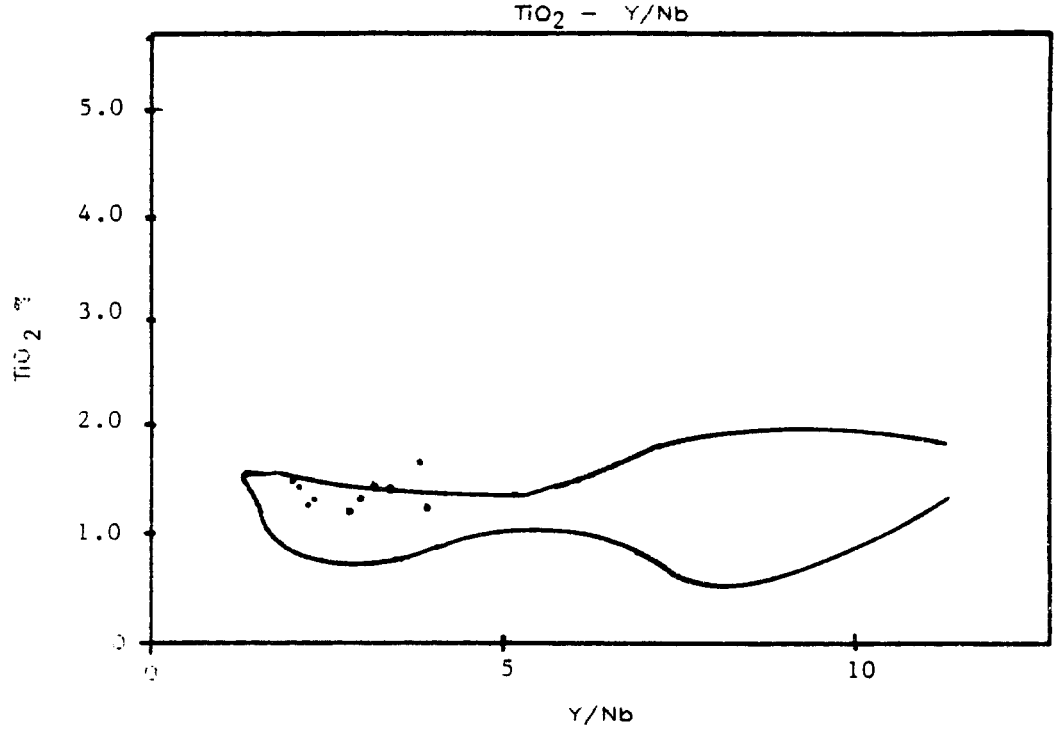

FLOYD—WINCHESTER PLOT

Nb/Y – Zr/P_2O_5

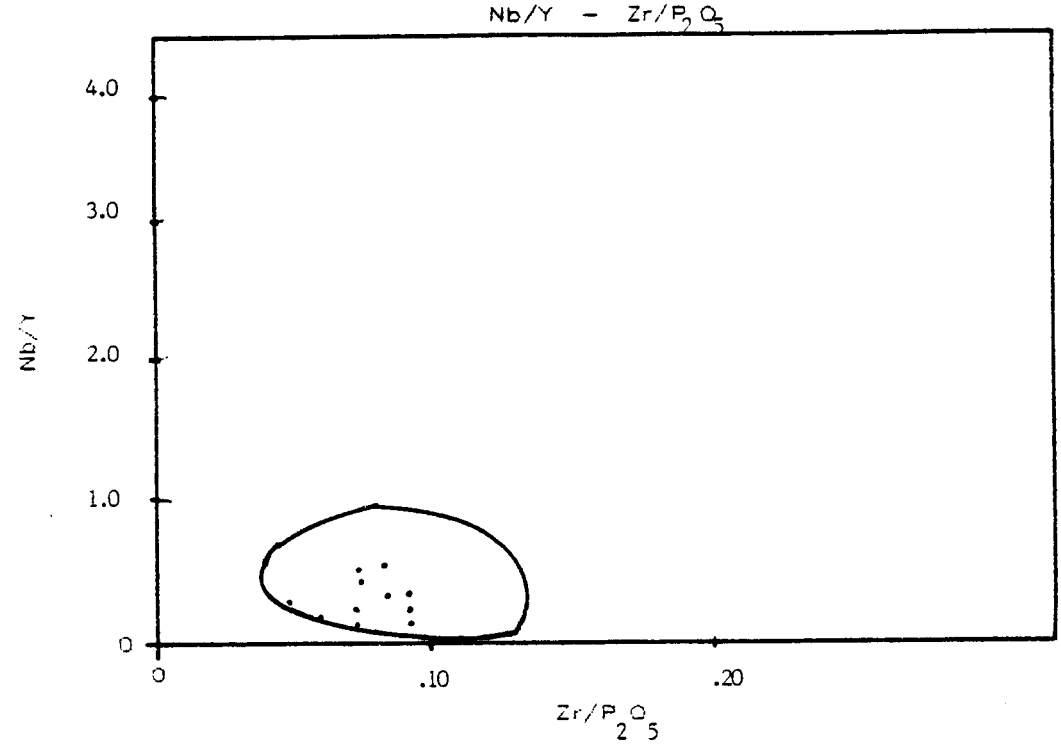

Figure 14c : TiO_2 vs Zr/P_2O_5 plot
with the oceanic thoeiite field of F&W (1975)

Figure 14d : P_2O_5 - Zr diagram of Floyd and Winchester (1975) showing delineated field of oceanic tholeiites

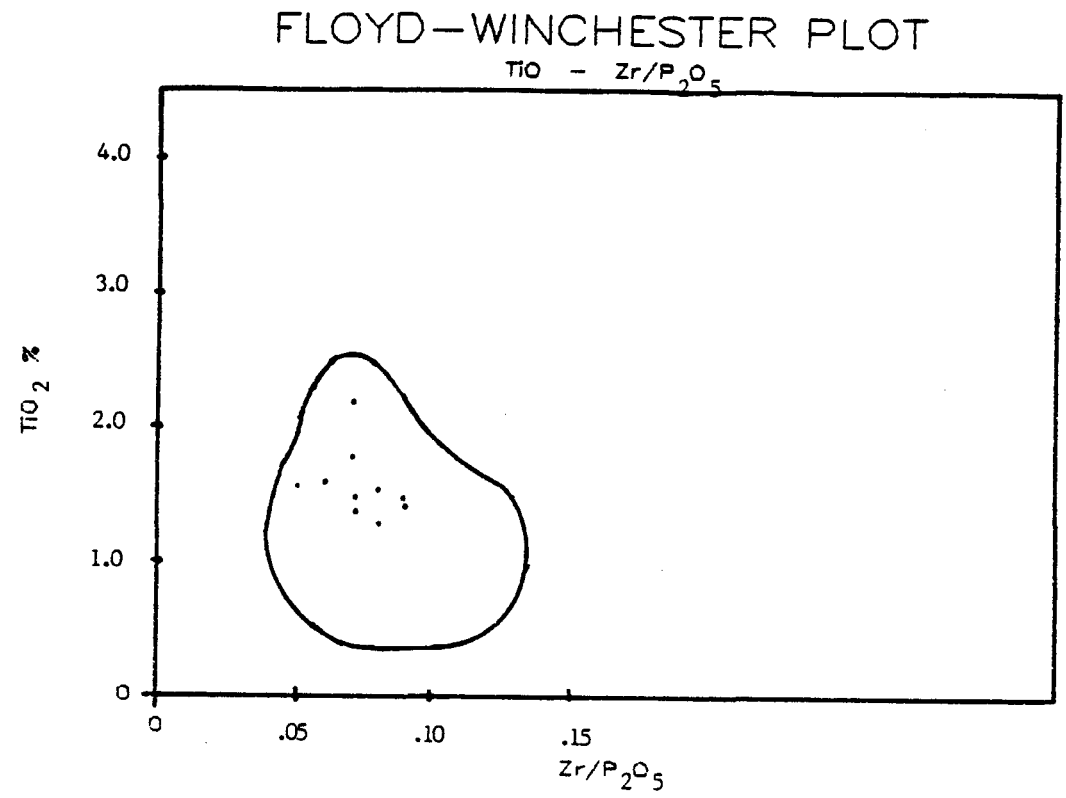
FLOYD—WINCHESTER PLOT
TiO - Zr/P2O5
4.0
3.0
2.0
1.0
0
TiO2 %
0
.05
.10
.15
Zr/P2O5

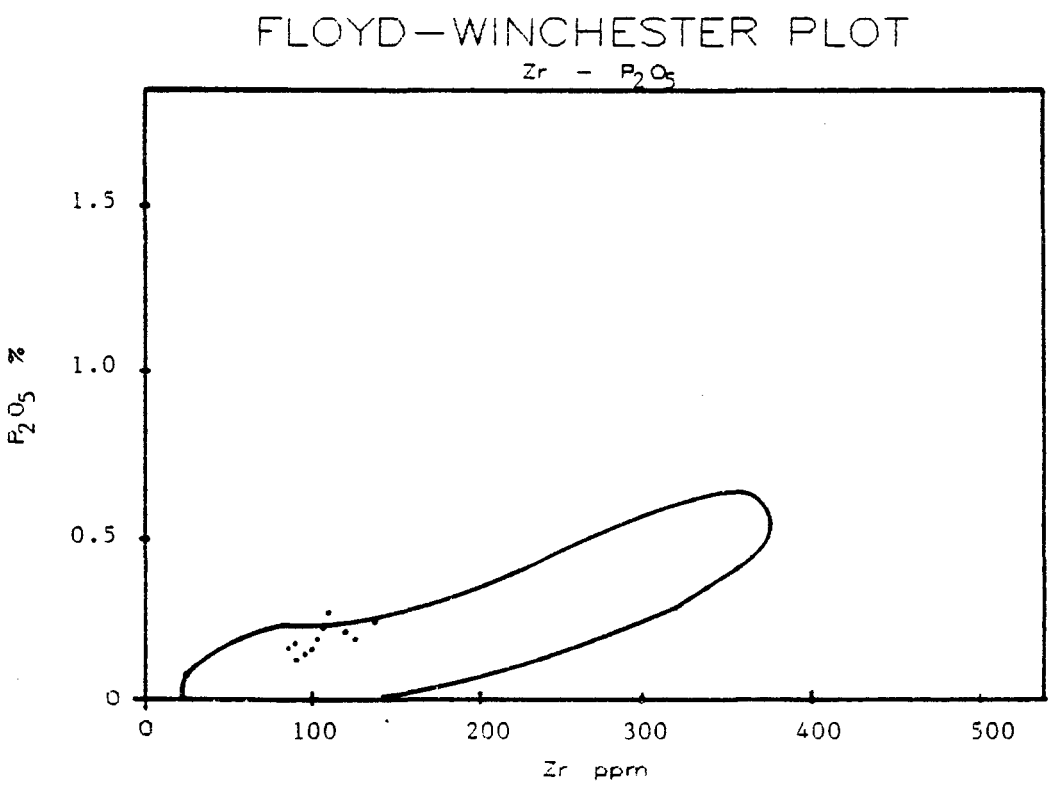
FLOYD—WINCHESTER PLOT
Zr - P2O5
1.5
1.0
0.5
0
P2O5 %
0
100
200
300
400
500
Zr ppm

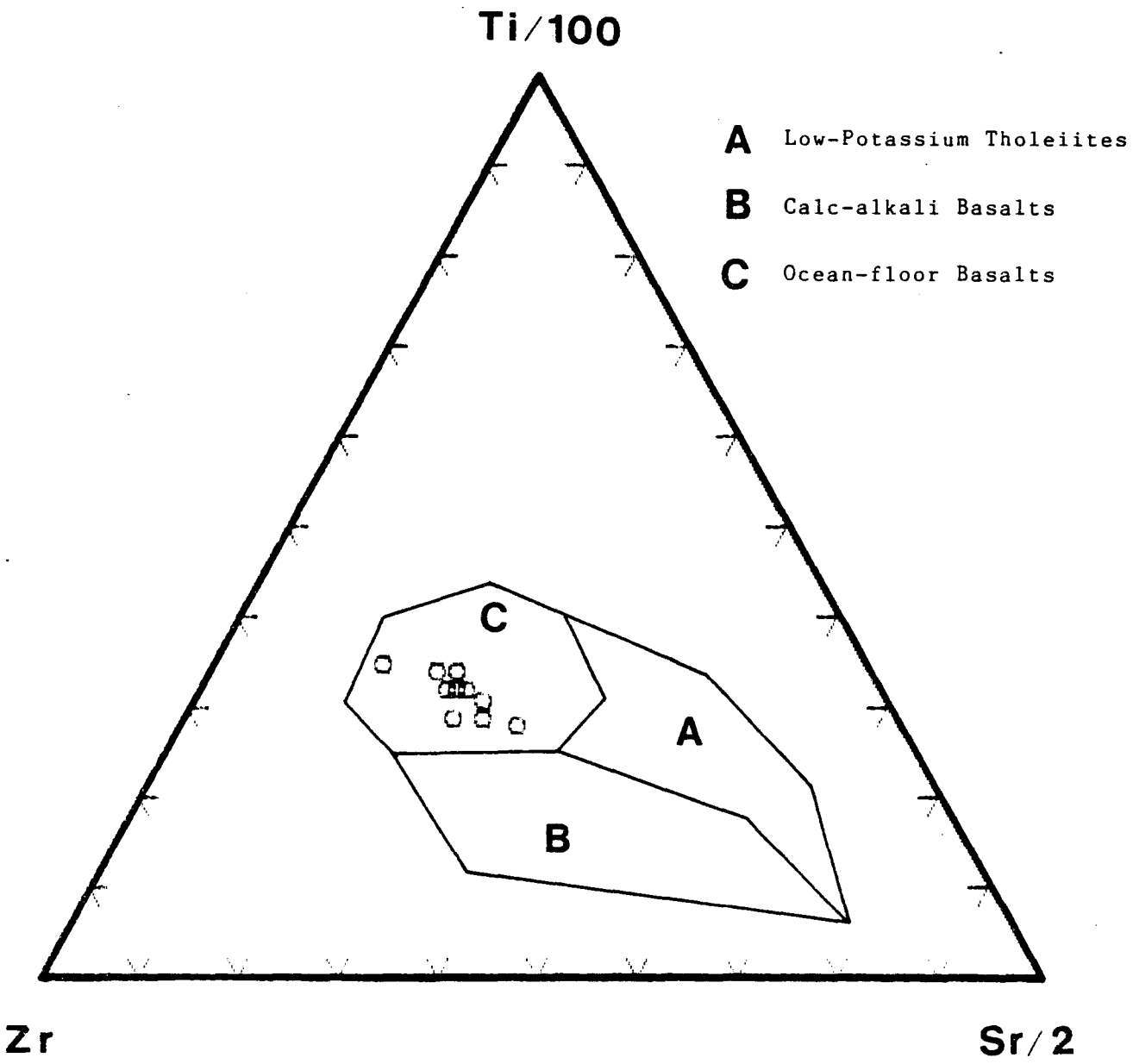

Figure 15: Discriminant Diagram using Zr, Ti and Sr (after Pearce and Cann 1973)

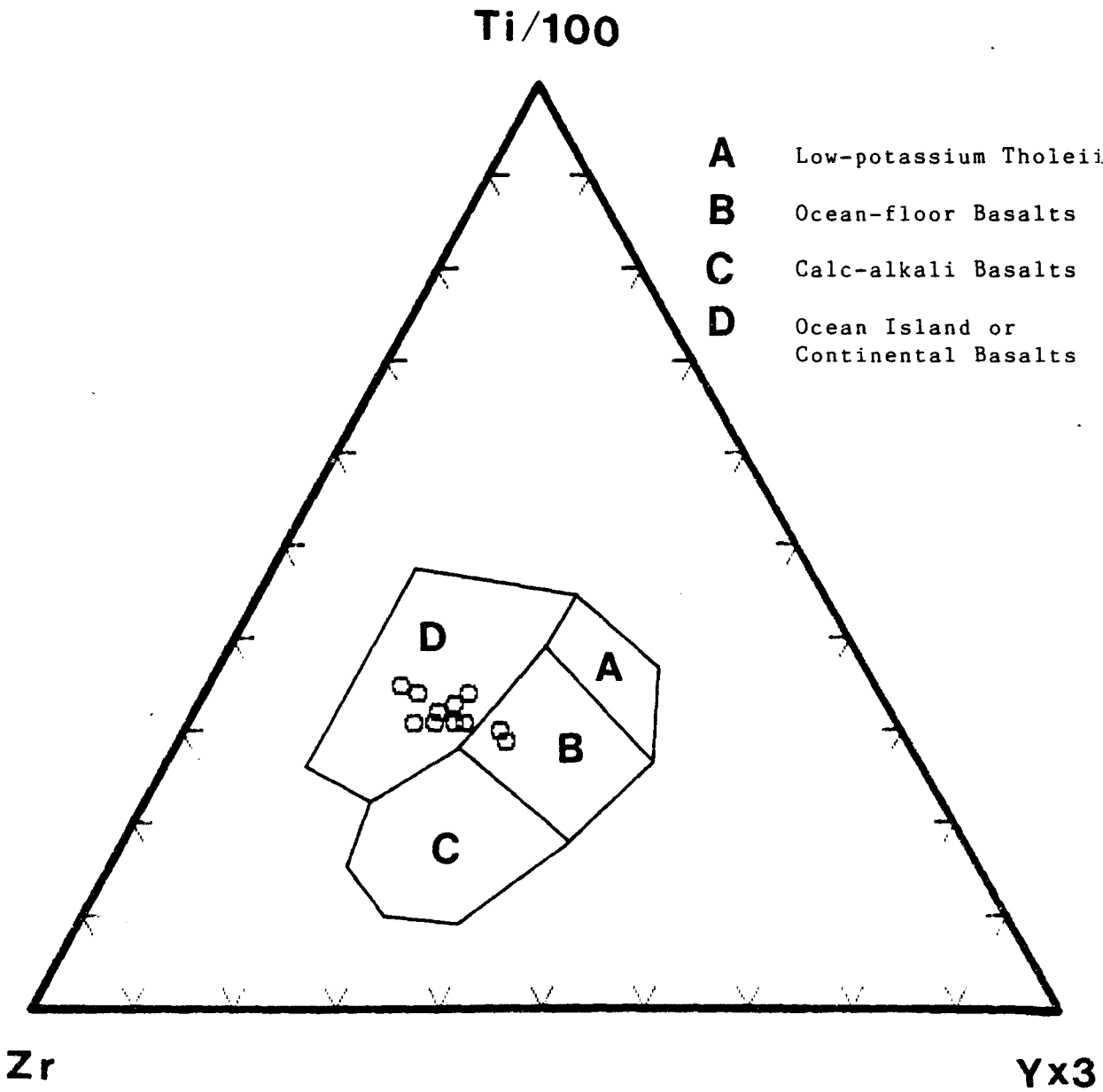

Figure 16: Discriminant Diagram using Zr, Ti and Y (after Pearce and Cann 1971)

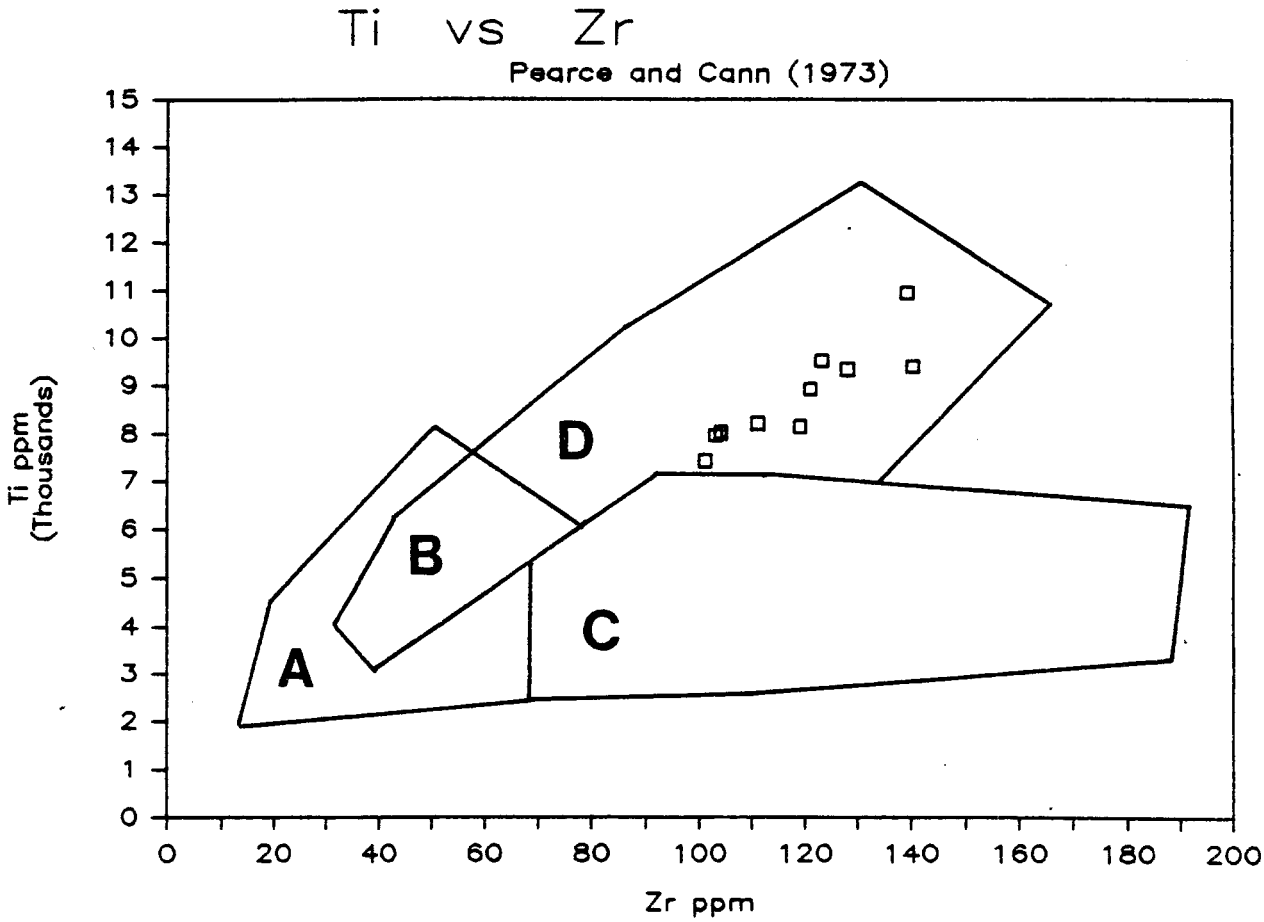

A Low-potassium Tholeiites

B Ocean-floor Basalts and Low-K Tholeiites

C Calc-alkali Basalts

D Ocean-floor Basalts

Figure17 : Discriminant Diagram using Ti and Zr (after Pearce and Cann 1971)

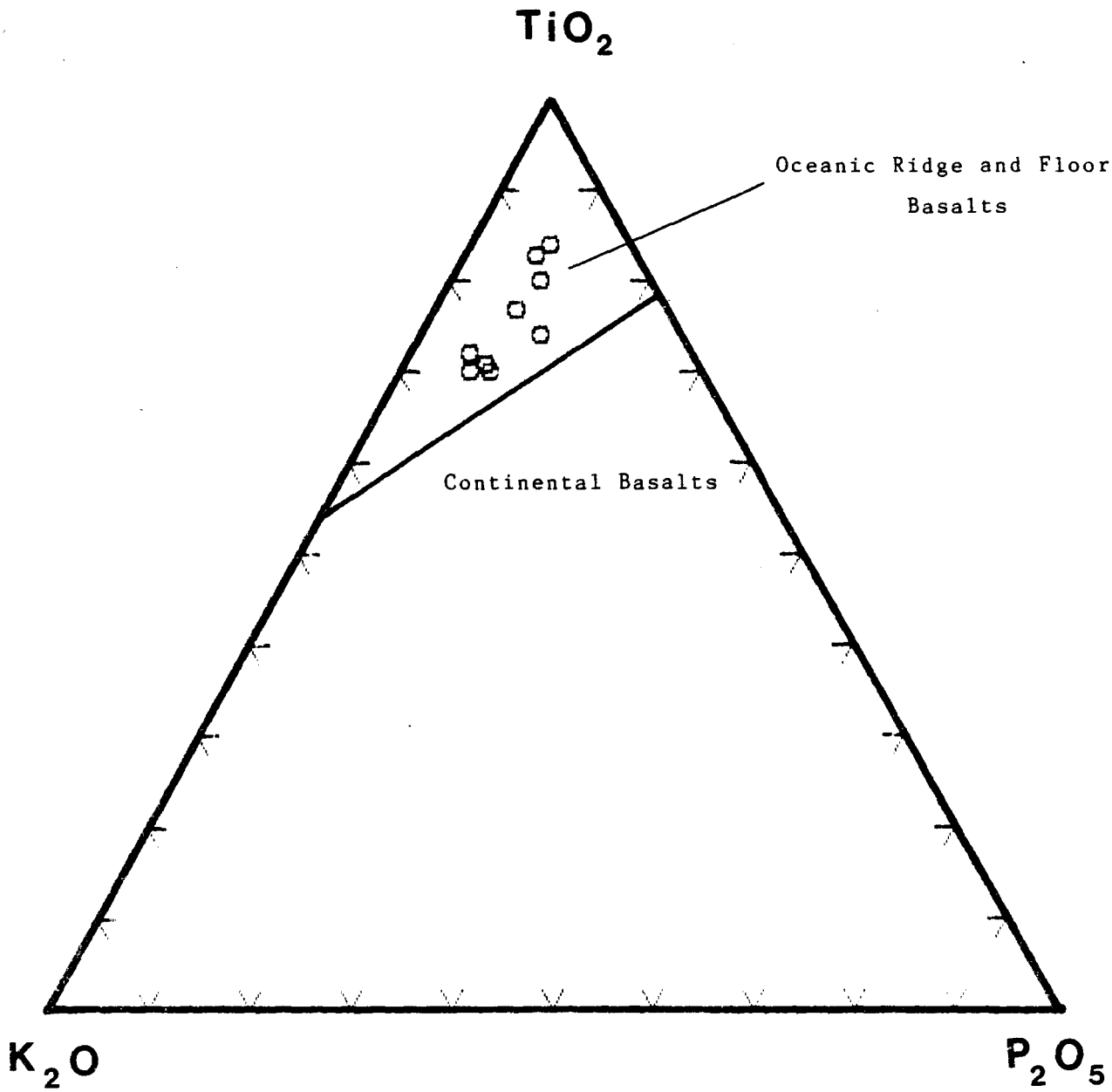

Figure 18: Discrimination Diagram using the major elements TiO_2, K_2O and P_2O_5 (after Pearce et al. 1975)

metasomatic alteration and therefore Y will likely be similiarly depleted. The Ti-Zr plot of Pearce and Cann (1973) once again shows all data points to fall within the ocean floor basalt field (figure17). The same conclusion is reached using the K_2O-TiO_2-P_2O_5 triangular plot (figure 18) of Pearce et al. (1975).

5.3 Conclusions

1) The preservation of primary igneous minerals such as clinopyroxene and olivine as well as the abundance and type of inclusions in the phenocryst phases are the most useful criteria with which to determine the degree of alteration in these basalts.

2) All samples have undergone low grade - greenschist facies metamorphism.

3) Depletion of Ca and Mg and an enrichment in K, P, Na, Si and H_2O has occured in the samples relative to fresh ocean-floor basalts.

4) Trace element data indicates that these basalts were originally oceanic tholeiites.

REFERENCES

AMSTUTZ,G.C. 1974. Spilites and spilitic Rocks. Springer-Verlag: 482 p.

BENSON,W.N. 1926. The tectonic conditions accompanying the intrusion of basic and ultrabasic igneous rocks. Nat. Acad. Sci. Mem. 19, No. 1: 90 p.

BISCHOFF,J.L.,DICKSON,F.W. 1975. Seawater-basalt interaction at 200 ^{o}C and 500 bars: Implications for origin of sea-floor heavy metal deposits and regulation of seawater chemistry. Earth Planet. Sci. Letters, 25: pp 385-397.

BRYAN,W.B. 1972. Morphology of quench crystals in submarine basalts. J. Geophys. Research, 77: pp 5812-5819.

BRYAN,W.B. 1972. Mineralogical studies of submarine basalts. Carnegie Institute of Washington, Geophysical Laboratory Annual Report: pp 396-403.

CANN,J.R. 1970. New model for the structure of the ocean crust. Nature, 226: pp 928-930.

CANN,J.R. 1970. Rb,Sr,Y,Zr and Nb in some ocean floor basaltic rocks. Earth and Planet. Sci. Letters, 10: pp 7-11.

CASEY,J.F.,KIDD,W.S.F. 1981. A parallochthonous group of sedimentary rocks unconformably overlying the Bay of Islands ophiolite complex, North Arm Mountain, Newfoundland. Can. J. Earth Sci., 18: pp 1035-1050.

CHURCH,W.R. 1972. Ophiolite: its definition, origin as oceanic crust, and made of emplacement in orogenic belts, with special reference to the Appalachians. Canada Dept. of Energy, Mines and Resources, Earth Physics Branch, Pub. 42, No. 3: pp 71-85.

COLEMAN,R.G. 1977. Ophiolites. Springer-Verlag, 229 p.

DEWEY,J.F.,BIRD,J.M. 1971. Origin and emplacement of the ophiolite suite: Appalachian ophiolites in Newfoundland. J. Geophys. Research, No 14. vol 76: pp 3179-3206.

DIETZ,R.S. 1963. Alpine serpentinites as oceanic rind fragments. Bull. Geol. Soc. Amer., 74: pp 947-952.

DUKE,N.A.,HUTCHINSON,R.W. 1973. Geological relationships between massive sulfide bodies and ophiolitic volcanic rocks near York Harbour, Newfoundland. Can. J. Earth Sci., 11: pp 53-69.

EINARSON,G.W. 1975. Low rank metamorphism in the Bay of Islands opiolite, western Newfoundland. G.A.C. Prog. and Abs.: p 752.

FLOYD,P.A.,WINCHESTER,J.A. 1975. Magma type and tectonic setting discrimination using immobile elements. Earth Planet. Sci. Letters, 27: pp 211-218.

FYON,J.A. 1980. Seawater alteration of early PreCambrian (Archean) volcanic rocks and exploration criteria for stratiform gold deposits, Porcupine Camp, Abitibi Greenstone Belt, Northeastern Ontario. Unpub. MSc Thesis, McMaster University: 238 p.

GASS,I.G.,SMEWING,J.D. 1973. Intrusion,extrusion and metamorphism at constructive margins: evidence from the Troodos Massif, Cyprus. Nature, 242: pp 26-29.

HART,S.R. 1970. Chemical exchange between sea water and deep ocean basalts. Earth Planet. Sci. Letters, 9: pp 269-279.

HART,S.R.,ERLANK,A.J.,KABLE,E.J.P. 1974. Sea floor basalt alteration: some chemical and Sr isotopic effects. Contrib. Min. and Pet., 44: pp 219-230.

HESS,H.H. 1964. The oceanic crust, upper mantle and the Magaguez serpentinized peridotite. Nat. Acad. Sci. - National Research Council Publ. 1188: pp 169-175.

HOWLEY,J.P. 1907. Geological map of Newfoundland. source not given.

HUGHES,C.J. 1973. Spilites, Keratophyres and the igneous spectrum. Geo. Mag., 109: pp 513-527.

IRVING,T.N.,BARAGAR,W.R.A. 1971. A guide to the chemical classification of the common volcanic rocks. Can. J. Earth Sci., 8: pp 523-548.

JOHNSTON,H. 1941. Paleozoic lowlands of western Newfoundland. Trans. New York Acad. Sci., ser. 2, vol. 3: pp 141-145.

KAY,M. 1945. Paleogeograhic and palinspastic maps. Bulletin Am. Assoc, Petrol. Geol., 29: pp 426-450.

KAY,R.W.,HUBBARD,N.J. 1978. Trace elements in ocean ridge basalts. Earth Planet. Sci. Letters, 38: pp 95-116.

LAURENT,R.,HEBERT,Y. 1977. Features of submarine volcanism in ophiolites from the Quebec Appalachians. GAC Special Paper 1

LOFGREN,G. 1971. Sperulitic textures in glassy and crystalline rocks. Journ. Geophy. Res., 76: pp 5635-5648.

MACKENZIE,W.S.,DONALDSON,C.H.,GUILFORD,C. 1982. Atlas of igneous rock textures. John Wiley and Sons. 128 p.

MALPAS,J.,TALKINGTON,R.W. 1979. Ophiolites of the Canadian Appalachians and Soviet Urals. Contributions to I.G.C.P. Project 39.

MALPAS,J.,STEVENS,R.K. 1977. The origin and Emplacement of the Ophiolite Suite with Examples from Western Newfoundland. Geotectonics, vol 11, No. 6: pp 453-465.

MALPAS,J. 1977. Petrology and tectonic significance of Newfoundland ophiolites, with examples from the Bay of Islands, in North American ophiolites ed. by R.G. Coleman and W.P. Irwin. Orogen Dept. of Geol. and Mineral Industries Bull. 95: pp 13-23.

MALPAS,J. 1978. Magma generation in the upper mantle, field evidence from ophiolite suites and application to the generation of oceanic lithosphere. Philisophical Transactions - Royal Society of London. Series A. 288: pp 527-546.

MALPAS,J. 1979. The dynamothermal aureole of the Bay of Islands Ophiolite Suite. Can. J. Earth Sci., 16: pp 2086-2101.

MARCHAND,M. 1973. Determination of Rb, Sr and Rb/Sr by XRF. Tech. memo 73-2, Department of Geology, McMaster University.

MELSON,W.G.,THOMPSON,G.,ANDEL,T.H. 1968. Volcanism and metamorphism in the Mid-Atlantic Ridge, 22N latitude. J. of Geophys. Res. 73: pp 5925-5941.

MOORE,J.G. 1965. Petrology of deep-sea basalts near Hawaii. Amer. J. of Sci, 263: pp 40-52.

MULLER,G.,STRAUSS,K.W. 1984. Mass Balance of Spilitization and of Similar Metasomatic Processes in Keratophyres and Picrites from Rhenohercynian Piles. Chemie der Erde, 43: pp 279-293.

PEARCE,J.A. 1975. Basalt Geochemistry used to investigate past tectonic environments on Cyprus. Tectonophysics, 25: pp 41-67.

PEARCE,J.A.,GORMAN,B.E.,BIRKETT,T.C. 1977. The relationship between major element chemistry and tectonic environment of basic and intermediate volcanic rocks. Earth Planet Sci. Letters, 36: pp 121-132.

PEARCE,J.A.,GORMAN,B.E.,BIRKETT,T.C. 1975. The TiO_2-K_2O-P_2O_5. Diagram: A method of discriminating between oceanic and non-oceanic basalts. Earth Planet Sci. Letters, 24: pp 419-426.

PEARCE,J.A.,CANN,J.R. 1973. Tectonic Setting of Basic Volcanic Rocks determined using Trace Element Analysis. Earth Planet Sci. Letters, 19: pp 290-300.

PEARCE,J.A.,CANN,J.R. 1971. Ophiolite origin investigated by discriminant analysis using Ti, Zr and Y. Earth Planet Sci. Letters, 12: pp 339-349.

RODGERS,J.,NEALE,E.R.W. 1963. Possible 'Taconic' Klippen in western Newfoundland. Amer. J. of Sci., 261: pp 713-730.

RONA,P.A. 1984. Hydrothermal mineralization at seafloor spreading centers. Earth Sci. Review, 20: pp 1-104.

SMITH,C.H. 1958. Bay of Islands igneous complex. C.G.S. Memo. 290: pp 132.

SPOONER,E.T.C.,FYFE,W.S. 1973. Sub-Sea-Floor Metamorphism Heat and Mass Transfer. Contr. Mineralogy and Petrology, 42: pp 287-304.

STANTON,R.L. 1972. Ore Petrology. McGraw-Hill, New York: pp 84-95.

STEINMANN,G. 1905. Geologische Beobachtungen in den Alpen II. Die Schardt'sche Uberfaltungstheorie und die geologische Bedeutung der Tiefseeabsatze und der ophiolithischen Massengesteine. Ber. Nat. Ges. Freiburg, 16: pp 44-65.

STEVENS,R.K. 1970. Cambro-Ordovician flysch sedimentation and tectonics in western Newfoundland and their possible bearing on a Proto-Atlantic Ocean. G.A.C. Spec. Paper, No. 7: pp 165-177.

STRONG,D.F. 1977. Volcanic regimes of the Newfoundland Appalachians. Geological Assoc. of Canada, Spec. Paper #16, Volcanic regimes in Canada.

STRONG,D.F. 1974. An 'off-axis' alkali volcanic suite associated with the Bay of Islands ophiolites, Nfld. Earth Planet Sci. Letters, 21: pp 301-309.

STRONG,D.F. 1973. Lushs Bight and Robert Arm Groups of Central Nfld.: Possible juxtaposed oceanic and island-arc volcanic suites. G.S.A Bulletin, 84: pp 3917-3928.

VALLANCE,T.G. 1974. Spilitic degradation of a tholeiitic basalt. Journal of Petrology, 15, Part 1: pp 79-96.

WELTON,J.E. 1984. SEM petrology atlas. Methods in exploration series. Ed. by R. Steinmetz. A.A.P.G. Tulsa, Oklahoma: 225 p.

WILLIAMS,H. 1975. Structural succession, nomenclature and interpretation of transported rocks in Western Newfoundland. Can. J of Earth Sci., 12: pp 1874-1893.

WILLIAMS,H. 1978. Appalachian Orogen in Canada. Can. J of Earth Sci., 16: pp 792-807.

WILLIAMS,H.,SMYTH,W.R. 1973. Metamorphic aureoles beneath ophiolite suites and alpine peridotites: Tectonic implications with West Newfoundland examples. Am. Journ. of Science, 273: pp 594-621.

WILLIAMS,H. 1973. Bay of Islands Map-Area Newfoundland. G.S.C. Paper 72-34.

WILLIAMS,H.,MALPAS,J. 1972. Sheeted dikes and brecciated dike rocks within transported igneous complexes, Bay of Islands, Western Newfoundland. Can. J of Earth Sci., vol. 9, No. 9: pp 1216-1227.

WILLIAMS,H. 1971. Mafic ultrmafic complexes in Western Newfoundland Appalachians and the evidence for their transportation: A review and interim report. G.A.C., Proceedings, vol. 24, No. 1: pp 9-25.

WILSON,J.T. 1966. Did the Atlantic close and then re-open? Nature 211: pp 676-681.

WINCHESTER,J.A.,FLOYD,P.A. 1976. Geochemical magma type discrimination: Application to altered and metamorphosed basic igneous rocks. Earth Planet Sci. Letters, 28: pp 459-469.

WINKLER,H.G.F. 1975. Petrogenesis of metamorphic rocks. Fifth edition. Springer-Verlag, New York: pp 168-201.

CRABB CREEK – BAY OF ISLANDS

Map made from 1:15,840 aerial photographs. Geology is as mapped by Duval with aerial-photo. interpretation based on maps by Williams 1972, Smith 1960, and Casey & Kidd 1981.

GEOLOGY

1 CRABB BROOK GP.; SUMMERHOUSE BK. FM.
JAWS BK. FM.
CRABB PT. FM.

2 Dominantly mafic pillowed lava often with silicic and/or calcitic alteration. Also mafic dykes increasing in numbers towards the base. Increasing in numbers towards the top are highly locally variable units of pillow breccia, agglomerate, conglomerate, and volcanoclastics. (these units when at the top are indistinguishable from the Crabb Pt. Fm.)

4c Granodiorite dykes minorly found within group 3. Probably originate as a source from group 4A and are chemically altered during intrusion of group 3.

4A Quartz-diorite unit; Probably a late stage siliceous and felsic phase of group 4 gabbro. Lithologies range in a patchy network from true quartz diorite through the intermediate stages to group 4 gabbro.

4B Amphibolite; Originally type 4A and 4, this unit is the product of dynamic metamorphism during thrusting, forming a layered or gneissic sequence of quartz diorite, gabbro and serpentinized ultramafic material. (also amphibolite & mica schist)

3 Sheeted dykes of diabase and mafic volcanics with variable amounts of alteration.

4 Gabbros medium to coarse grained and commonly altered.

Geology not shown.

LEGEND

- Plunging anticline, plunging syncline, anticline. (length of arms indicate relative dip of limbs, shorter being steeper.)
- strike & dip of bedding.
- schistosity or gneissic layers.
- attitude of dykes.
- attitude of shear zone.
- axis of minor folding.
- ? – lack of data indicating questionable.
- fault, defined or assumed.
- contact, defined or assumed.
- crest of ridge.

SCALE

1:15,840 1 inch = 1/4 mile.

Scale 1:250,000

BAY OF ISLANDS

THESIS AREA

GREGORY RIVER

ROCKY BROOK

STEEP BROOK

JAWS BROOK

UPPER CRABB BROOK

SUMMERHOUSE BROOK

LOWER CRABB CREEK

LIVERPOOL BROOK

N

mag. declination 27°13′west

BAY OF ISLANDS

DUVAL INTERNATIONAL CORPORATION	PROVINCE NFLD
CRABB CREEK	N.T.S. 12G/8
TYPE GEOLOGY	TOWNSHIP & RANGE Bay of Islands
DRAWN: M.LANGDON CHECKED: M.LANGDON DATE: 1/30/84	MAP No. 1B
	PLATE No.